Fermi National Accelerator Laboratory

FERMILAB-Pub-79/13-EXP
2125.000

(Submitted to Nucl. Instrum. Methods)

THE SEGMENTED CALORIMETER: A STUDY OF HADRON SHOWER STRUCTURE

A. L. Sessoms,* M. S. Goodman, L. Holcomb,
E. S. Sadowski, and A. Strominger
Physics Department and High Energy Physics Laboratory†
Harvard University, Cambridge, Massachusetts 02138

and

B. Eisenstein, L. E. Holloway, and W. T. Wroblicka
Physics Department,† University of Illinois at Urbana/Champaign
Urbana, Illinois 61801

and

S. C. Wright‡
Enrico Fermi Institute
University of Chicago, Chicago, Illinois 60637

and

R. D. Kephart
Fermi National Accelerator Laboratory, Batavia, Illinois 60510

January 1979

*Alfred P. Sloan Foundation Fellow
†Supported in part by the U. S. Department of Energy
‡Supported in part by the U. S. National Science Foundation

ABSTRACT

We describe the construction, operating characteristics, and use of a large segmented liquid argon/iron ionization calorimeter. With this instrument we have carried out quantitative studies of the development of hadronic showers at high energies. Results on both the longitudinal and transverse development of showers are given. The energy of an incident hadron can be determined with a resolution of:

$$\frac{\sigma_E}{E} = (8.5 + \frac{28}{\sqrt{E_H}})\%$$

and its direction with a resolution of:

$$\sigma_\theta = (16 + \frac{433}{E_H}) \text{ mrad}$$

INTRODUCTION

We have built and used a large segmented liquid argon/iron hadron calorimeter[1] (LARC). With it we have measured the direction and energy of hadron induced showers. The instrument is simple to calibrate absolutely, and monitoring the calibration continuously is straightforward. The capabilities and operating characteristics of this type detector make it well suited for accelerator neutrino experiments where the interaction rates are not large. The fine sampling of this device makes possible detailed studies of the structure of hadronic showers at high energies.

In the following sections we give the basis for the design, the mechanical construction, the temperature control system, the electronics, and the online readout of the calorimeter. Then the running conditions and event selection used in the hadron beam study are given. Finally the hadron shower characteristics and the energy and angular resolutions attained are described.

DESIGN BASIS

This calorimeter was designed to measure with high resolution both the energy and direction of hadrons. In our design we took into consideration possible sources of

fluctuations which limit the attainable resolution[2-4].

Since most of the energy in hadron showers ends up in an electromagnetic form[2] the sampling step was matched to the average radiation length of the calorimeter material. The elemental step size in our detector of 3 mm iron and 4 mm liquid argon is 0.2 radiation lengths.

Sampling fluctuations are associated with the fact that the energy deposition is only periodically sampled. In our design the fraction of energy deposited in the liquid argon is 0.2 of the total. We note that even in detectors designed to be homogeneously sensitive dead regions often represent a source of similar fluctuations.

Noise and statistical fluctuations in numbers of photons or ion pairs are other potential limits on resolution in calorimeters. The large number of ion pairs formed in liquid argon eliminate statistical fluctuations. While the total amount of collected charge per channel is small (30 fC for a minimum ionizing particle) we were able to design an inexpensive ($20/channel) amplifier-readout system that could cleanly resolve this signal above noise background.

A scheme for calibration, both overall and between various sections of the calorimeter, is designed into the system. The ability to resolve single minimum ionizing particles

gives us an additional absolute calibration method.

Finally, we note that in contrast to some other techniques a liquid argon ionization chamber has highly uniform response over its entire extent.

We summarize some of the important design features of our calorimeter in the following list:

1. very small sampling step
2. low noise amplifiers
3. uniformity of response and ease of calibration
4. high average density (4.17 gm/cm^3)
5. low cost per unit mass.

DESIGN

Our calorimeter consisted of solid steel high voltage plates, 60 cm x 60 cm x 3 mm . a 4 mm liquid argon gap, and a 60 cm x 60 cm signal electrode made up of steel strips 60 cm x 2 cm x 3 mm, followed by another 4 mm liquid argon gap. This was repeated throughout the device with strips of horizontal (y) and vertical (x) orientation alternating with each other. The configuration is shown schematically in

Figure 1.

The steel plates and strips were electroplated with approximately 10 microns of copper. This assured cleanliness and was useful since all connections to the strips and plates were made with solder. The strips and plates were separated by G-10 spacers 50 cm x 1 cm x 4 mm. These spacers were notched so that the strips could be cemented in place with a 1 mm spacing between them. This space was necessary in order to minimize the cross coupling between strips.

The spacers were attached to the plates and strips with CREST 7410 cryogenic epoxy[5]. This epoxy has excellent properties and could be relied upon to hold under the stresses of cool down and operation at liquid argon temperatures.

The modules were placed in a support frame made of an aluminum substructure and a G-10 superstructure. The strips were ganged together longitudinally in groups of five and coupled to amplifiers through low inductance 30 conductor ribbon cable[6], each signal wire alternating with a ground wire. Thus each wire read out five longitudinally consecutive samples in x or y; we call this a section.

We had, in effect, 12 planes with two-dimensional readout.

Each plane comprised a total of 0.7¾ interaction lengths (3.52 radiation lengths). Due to the interleaving of x and y electrodes within each plane the amount of charge collected in each section corresponds to one-half of that deposited by the shower. The readout of each of the 696 sections corresponded to 2 cm of iron transverse to the shower direction. Details of the calorimeter are given in Table 1.

CRYOSTAT AND COOLING SYSTEM

The module assembly rested in a double-walled vacuum insulated Dewar to cut heat gain to a minimum. All connections from the liquid argon environment to the outside were through warm seals; this made the vacuum seals relatively straightforward. The signal cables, liquid nitrogen connections, argon fill tubes, gaseous argon lines, and vacuum assemblies were brought out through stainless steel vacuum insulated feed-through connectors.

The inner cryostat was stainless steel. There were several attempts using indium to make the vacuum seal on this tank. This proved to be impossible with the size flanges used because during cool down the tank would contract, thus compressing the indium; during operation the pressure was positive, thereby pushing the flanges apart. No amount of

tightening after recycle could assure a trustworthy seal. In the end, the standard technique of welding the seams was successfully employed.

The outer tank was of carbon steel; the space between the two tanks was filled with several layers of super insulation and evacuated. The outer Dewar remained at room temperature during the study.

The cooling system consisted of a curved perforated copper sheet suspended inside the inner Dewar above the calorimeter module, and extending over its length and width. Soldered to the sheet was 0.5 inch inside diameter copper tubing through which liquid nitrogen was allowed to flow. This copper cooling shroud was sufficient to cool the entire detector down to liquid argon temperatures and to maintain the temperature at that level during operation. The temperature was monitored by a thermometer[7] that is accurate to 0.1° C in the range around -200° C.

The temperature, pressure, and purity of the argon in the calorimeter were maintained in the following way. The calorimeter was cooled down to -185° C by flowing liquid nitrogen through the cooling shroud. Liquid argon was then transfered into the calorimeter through vacuum insulated transfer lines from commercial 160 liter containers. The purity of the liquid argon was continuously monitored by an

oxygen meter[8]. The commercially purchased liquid was pure to approximately 1 part per million oxygen contamination and remained so without purification. Once the Dewar was filled (approximately 600 liters of liquid argon) a temperature control system was activated. This system sensed the argon vapor pressure in the inner Dewar. When this pressure reached 6 lbs./sq. in., liquid nitrogen was permitted to flow through the cooling shroud. When the pressure fell below 2 lbs./sq. in. the flow was stopped. This was found to be a stable system which gave no problems throughout the experiment. A schematic diagram of the system used for this study is shown in Figure 2.

ELECTRONICS

A block diagram of the electronics is shown in Figure 3. Briefly, a trigger was generated by scintillation counters which started the central circuitry. Signal G_1 was generated immediately; it opened a switch that allowed the integrate and hold circuits to collect charge from the calorimeter. At a later time, chosen to be between 1 and 4 microseconds, signal G_2 was generated which decoupled the amplifiers from the integrate and hold circuits. The data were ready to be read out at this point. The computer (not shown, but in this case a PDP 11/20) initiated a read cycle through a CAMAC Read In/Read Out Digital to Analog Converter

(RIRODAC)[9]. The 696 d.c. levels were then presented through a multiplexing system to CAMAC analog to digital converters[10]. The multiplexing was such that 36 ADC channels contained in 3 standard CAMAC modules accomodated all the data. A circuit diagram of the electronics is given in Figure 4.

To reduce the number of separate cards and the amount of external wiring required the amplifiers, integrate and hold circuits, and multiplexers were packed 60 channels to a single card. Only 58 channels were used for data taking. Each card had its own voltage regulator for ±15 volts, and ±5 volts in order to isolate them from fluctuations in power supply voltage. This also added a layer of noise isolation. The electronics was mounted directly on the top shell of the Dewar and only 36 signal wires went from the calorimeter to the experiment control room. A photograph of a 60 channel board is shown in Figure 5.

It is interesting to note the ease of calibration and monitoring of this system. The gain of each amplifier could be monitored continuously during the data taking cycle. A series of numbers were written into the RIRODAC by the computer; the RIRODAC responded by sending a d.c. level corresponding to this number to the input of all channels simultaneously (see Figure 4). In addition it generated a signal which looked like a trigger and gated in this level.

The normal read sequence followed and this "test pulse" data was stored and monitored. The linearity and stability of the electronics was measured every 10 seconds. By comparison any device utilizing other methods for calorimetry (lead glass, lead or iron scintillation calorimeters, flash chambers, multiwire proportional chambers, etc.) must employ enormously more complicated, less reliable, and more pedestrian techniques to achieve this goal.

The total readout time for 720 channels using a PDP 11/20 computer and BD-011 CAMAC parallel branch driver was 4 milliseconds. A calibration curve for a single channel of electronics is given in Figure 6. A minimum ionizing particle corresponds to approximately 8 ADC counts in one section (pedestal subtracted) on the scale shown. A typical 20 GeV shower contains 50 particles at its peak, or about 400 counts.

RUNNING CONDITIONS

This study was carried out in the M-5 beam at the Fermi National Accelerator Laboratory (FERMILAB). The beam was primarily negative pions with a small component of muons and electrons. The energies used ranged from 10 to 38 GeV. A Cerenkov counter in the beam served to tag particles as π/μ or e, and signals from a scintillation counter placed downstream of the calorimeter behind 3 meters of concrete tagged muons. The intensity was about 5000 particles/second; the accepted event rate was 20 per second. The total data taking time was 3 weeks.

The potential difference across the 4 mm liquid argon gap was 3.2 kV. At this potential difference the drift time per unit length was 180 ns/mm. The gains in the electronics were set so 1 ADC count corresponds to 3×10^{-15} coulombs (3 femtocoulombs).

MINIMUM IONIZING PARTICLES

A good test of a calorimeter's sensitivity is its ability to see single minimum ionizing particles (muons) traversing a single section. Figure 7 shows such a muon signal for a section lying on an average muon trajectory. These data were taken directly from the online computer display. The

muon signal is clearly resolved above the noise broadened pedestal.

EVENT SELECTION

The Cerenkov counter was less than 50% efficient; this led to substantial electron contamination in the hadron sample. In order to reduce this contamination to a reasonable level, we demanded that the interaction take place after the first 4 radiation lengths (r.l.) of the calorimeter, i.e., the first x and y planes were not used as a source of events in the final data sample. With this cut electron contamination in the data sample was negligible.

In some previous studies with hadron calorimeters, event selection criteria were made to insure total containment of the shower. These criteria may favor events like $\pi^- p \to \pi^0 n$ and give optimistic results because of the better resolution for events that are primarily electromagnetic in origin[4]. Such event selection is not possible in normal experiments and so should not be used in studies of the kind discussed here. The only selection criterion applied to our data was that the incoming particle not be an electron or muon.

HADRON SHOWER CHARACTERISTICS

In studying a shower in an ionization calorimeter one measures the total charge deposited in the ionizing medium. This quantity is directly proportional to the total shower energy as will be seen in our subsequent discussion of chamber linearity.

Raw data for hadron showers as they appear in our single event online display are shown in Figures 8, 9, and 10. The hadron energies are 20, 30 and 38 GeV. A 30 GeV electron shower is shown in Figure 11. There is a clear distinction between the two types.

The profile of an average hadron shower is determined by summing over a large number of events and normalizing to the total. Such an average is shown in Figure 12 for the 20 GeV data. The coordinates are Z, the length along the shower in plane numbers, and X, the projected distance from the shower axis in section numbers. The vertex occurs in "plane" 2; in "plane" 1 the signal is due to the incoming minimum ionizing particle. The shower peaks in "plane" 3 (which is 0.74 interaction lengths from the vertex)[11] and it finally dies out in "plane" 8. The envelope of the shower, that is the width that contains greater than 99% of the visible energy in each plane, is football shaped (American style). This width is plotted in Figure 13 as a function of energy. We

can parametrize the width, W(E), at the shower peak by

$$W(E) = -17.28 + 14.28 \ln E \text{ (GeV)} \qquad (1a)$$

or

$$W(E) = -4.03 + 6.39 \sqrt{E} \quad \text{(GeV)} \qquad (1b)$$

W(E) is in centimeters. Both functional forms fit the data reasonably well.

Another aspect of the lateral spread of the shower is illustrated in Figure 14 where the total charge in the x-view of the calorimeter is plotted as a function of position across the face of the shower. We define the projected transverse shower distribution as:

$$I(X) = \sum_{j=1}^{12} Q_{ij}^{X}$$

where Q_{ij}^{X} is the charge collected in section i of the j-th X-plane and X is the distance from the shower axis to the i-th section. Figure 15 shows the energy dependence of the full width at half maximum of this distribution. The increase in the lateral spread as a function of energy is small.

The longitudinal energy deposition of the shower is shown in Figure 16, a plot of the measured charge as a function of shower depth. The mean depth of the energy deposition moves with energy and can be fit by the form:

$$Z_{mean}(E) = 0.90 + 0.36 \ln E \ (GeV)$$

where Z_{mean} is in interaction lengths. Note that there are long tails extending several interaction lengths beyond the peak of the shower.

The integral energy deposition as a function of sampling depth in the calorimeter is plotted in Figure 17. It is interesting to note that almost total containment of the showers occurs in the first five interaction lengths for all our energies. The plateaus are fairly flat and the approach to them is sharp. Defining L as the thickness of absorber beyond which less than 10% of the energy remains, we find :

$$L = -1.26 + 1.74 \ln E \ (GeV) \qquad (3)$$

This "length of the shower" is given in interaction lengths.

LINEARITY AND ENERGY RESOLUTION

The Fermilab beam is on for 1 second out of 10. Before each of these "bursts" the pedestal (the sum of the d.c. offset and steady state noise) for each section was recorded. For each event, in order to ascertain the true pulse height, each section has the average value of its pedestal subtracted. The "total pedestal", summed over all

amplifiers in LARC, was found to be stable over many events in a run, and from run to run. The average value of this sum was 1.86×10^4. The shape of the distribution was Gaussian with a standard deviation of 4.00×10^2. The width of this distribution has not been subtracted from the width of the total pulse height distribution in the determination of the energy resolution.

The linearity of the system was determined by the 10, 20, and 30 GeV points. A plot of most probable pulse height versus energy is shown in Figure 18. The beam was then tuned to the highest possible momentum which, due to magnet saturation, was uncertain. From the calorimeter signals and a linear energy extrapolation the momentum was determined to be 38 GeV. This point is shown as an open square in Figure 18. The first three points of this plot show the direct linear relationship between the amount of the charge deposited in LARC and the energy of the incoming particle.

In order to measure the energy resolution of this device, we assumed that the incident hadron beam was monochromatic. Then the standard deviation of the measured energy corresponded to the energy resolution. In fact the conditions of the beam line during our data taking were far from ideal; energy loss and straggling caused by obstructions in the beam line were serious. This forces us to regard the energy resolutions we have determined as upper

limits. A plot of σ_E/E is given in Figure 19. We have also plotted the data of Fabjan, et al[2]. The fit to the combined data is $\sigma_E/E=(8.5+28/\sqrt{E})\%$. The data are not consistent with a simple $\sigma_E/E=A/\sqrt{E}$ dependence; the nonzero constant term is forced by the fit and dominates the resolution above 30 GeV.

ANGULAR RESOLUTION

We see from Figures 8, 9, 10 and 11 that the position of a shower, e.g., its centroid, is known to better than the width of a section. The angular resolution depends on how well the calorimeter is aligned, section to section, and on shower fluctuations. The latter is the dominant factor limiting the resolution.

Projected shower angles have been calculated in two independent ways. In the first case, centroids were found for the charge distributions in each "plane" downstream of the vertex. Each centroid had an error associated with it and a straight line was fit through these points. No other cuts were made. In the second case we determined an energy weighted average over all sections in the calorimeter downstream of the vertex. The results are the same for the two methods. In either case the incident beam dispersion was taken as zero and the standard deviation of the reconstructed angular distribution was assumed to measure

the angular resolution. The result of this analysis is shown in Figure 20, along with the functions

$$\sigma_\theta = 114(1.0 - 0.21 \ln E) \text{ mrad}$$

and

$$\sigma_\theta = (16 + \frac{433}{E}) \text{ mrad}$$

We cannot distinguish between these two functional forms over the energy range studied in this experiment.

CONCLUSIONS

A large, finely segmented liquid argon/iron hadron calorimeter has been used to study hadron shower characteristics. The calorimeter proved simple to calibrate and maintain; argon purity was not a problem and no purification was necessary.

It has been shown that the width of the envelope of the shower peak increases with energy and is described by the functions

$$W(E) = -17.28 + 14.28 \ln E$$

or

$$W(E) = -4.03 + 6.39 \sqrt{E}$$

where E is in GeV and W(E) is in centimeters.

The mean depth of the energy deposition has been shown to behave as

$$Z_{mean}(E) = 0.90 + 0.36 \ln E$$

in interaction lengths. The "total length" of the shower can be parametrized as:

$$L = -1.26 + 1.74 \ln E$$

in interaction lengths. The energy resolution of the calorimeter is fit by

$$\frac{\sigma_E}{E} = (8.5 + \frac{28}{\sqrt{E}})\ \%$$

A simple $A/\sqrt{E}$ dependence does not fit the data. It should be noted that pure liquid scintillator calorimeters have energy resolutions that show little or no energy dependence in this energy region[12]. The energy resolution found here falls between the two extremes of the coarse iron/scintillator and the pure liquid scintillator calorimeter.

The angular resolution of the calorimeter is consistent with either of the forms:

$$\sigma_\theta = 114(1.0 - 0.21 \ln E) \text{ mrad}$$

or

$$\sigma_\theta = (16 + \frac{433}{E})$$

ACKNOWLEDGMENTS

We are indebted to the staffs of the Harvard University High Energy Physics Laboratory, the Enrico Fermi Institute of the University of Chicago, and Research Services of Fermilab for invaluable help in carrying out this project. We are especially indebted to W. Dunn, J. Kinoshita, J. McElaney, M. Robbins, R. Haggerty, and J. O'Kane of HEPL.

Two of us (ALS and MSG) would like to thank Prof. Richard Wilson for his support during various phases of this work.

REFERENCES

1. A.Strominger, A.L.Sessoms, E.S.Sadowski, M.Robbins, and L.Holcomb, IEEE Transactions in Nuclear Science, NS 25 (1978) 354.

2. C.W.Fabjan et al., Nuclear Instruments and Methods, 141 (1977) 61.

3. M.Holder et al., to be published.

4. W.J.Willis and V.Radeka, Nuclear Instruments and Methods, 120 (1974) 221: See also:

   J.Engler, et al., Nuclear Instruments and Methods, 120 (1974) 157;

   G.Knies and D.Neuffer, Nuclear Instruments and Methods, 120 (1974) 1;

   T.A.Gabriel, and W.Schmidt, Nuclear Instruments and Methods, 134 (1976) 271;

   D.Hitlin, et al., Nuclear Instruments and Methods, 137 (1976) 225;

   W.Hofmann, et al., Nuclear Instruments and Methods, 135 (1976) 51;

   W.Selove, et al., in the "Proceedings of the Fermilab Calorimeter Workshop", M.Atac, ed. May 1975;

   H.Hilscher, et al., ibid.;

   V.Eckardt, et al., Nuclear Instruments and Methods, 155 (1978) 389.

5. Manufactured by CREST Products Corp., Santa Ana, California.

6. Manufactured by Electroweave, Inc., Worcester, Mass. This cable must be used with caution. It is not gas tight.

7. Manufactured by Analogic, Inc., Wakefield, Mass.

8. Manufactured ΔF Corp., Woburn, Mass.

9. This device was designed and built at Harvard and has been used in other applications. See for example A.L.Sessoms, E.S.Sadowski and L.Holcomb, IEEE Transactions in Nuclear Science, NS-25 (1978) 38; L.Holcomb and A.L.Sessoms, Nuclear Instruments and Methods 144 (1977) 597.

10. 11 Bit LeCroy 2259A analog to digital converters. Manufactured by LeCroy Research Systems, Inc., West Nyack, New York.

REFERENCES (Cont'd.)

11. For convenience, we have chosen to measure z from the upstream face of the calorimeter. The (primary interaction) vertex of the shower is, by selection, in plane 2. The vertex cannot be localized precisely in z because of the finite thickness of one plane, and has in all cases been assumed to lie at the center of plane 2, whose z-coordinate is 1.0 interaction lengths.

12. L.Sulak in the "Proceedings of the Fermilab Calorimeter Workshop", M.Atac, ed. May 1975.

TABLE I

LIQUID ARGON CALORIMETER

Active dimensions	60 x 60 x 175 cm
Sampling Step	3.0 mm iron (2.36 gm/cm^2) 4.0 mm liquid argon (0.56 gm/cm^2)
Electronic readout step:	
transverse (section)	2.0 cm
longitudinal (plane)	14.0 cm x and y steps interleaved
Target thickness	705 gm/cm^2
Target weight	2.7 tons
Channels of electronics	696
Average quantities	
density	4.17 gm/cm^3
radiation length	3.52 cm
interaction length	19.0 cm
Quantities per readout step:	
radiation lengths	3.52
interaction lengths	0.74
Total length	12 x and 12 y interleaved readout steps
radiation lengths	42.2
interaction lengths	8.6

FIGURE CAPTIONS

Figure 1: Schematic diagram of the calorimeter configuration.

Figure 2: Schematic diagram of the cryogenic system.

Figure 3: Block diagram of the electronics. The RESET signal from the RIRODAC served as the trigger to gate in the test level.

Figure 4: Circuit diagram of electronics showing one amplifier, integrate and hold, and multiplexing circuit. The measured droop of the holding capacitor was 1% in 8 ms. The total readout time for the system of 720 channels was 4 ms.

Figure 5: Photograph of a 60 channel electronics card showing amplifiers, integrate and hold circuits and voltage regulators. Only 58 channels on each card were used for data acquisition.

Figure 6: Typical calibration curve for a single channel of liquid argon electronics. Test pulse level is the number written into

the RIRODAC. A minimum ionizing particle corresponds to 8 ADC counts.

Figure 7: Pedestal and muon signals as seen by a single channel of electronics.

Figure 8: Typical shower for a 20 GeV hadron. Each horizontal line is 4 cm. Each vertical line represents one plane. The signal shown is in ADC counts divided by five.

Figure 9: Typical shower for a 30 GeV hadron. The signal is ADC counts divided by four.

Figure 10: Typical shower for a 38 GeV hadron. The signal is ADC counts divided by five.

Figure 11: Typical shower for a 30 GeV electron. The signal is ADC counts divided by ten.

Figure 12: Average shower distribution for 20 GeV hadrons with vertices in plane 2. A single pion signal is seen in plane 1.

Figure 13: Width of shower envelope vs. longitudinal position.

Figure 14: Transverse shower distribution as a function of x for 20 GeV hadrons. The distribution is symmetric and is similar for 10, 30, and 38 GeV incident hadrons.

Figure 15: Energy dependence of the FWHM for the transverse shower distribution.

Figure 16: Energy deposition as a function of the longitudinal position.

Figure 17: Integral energy deposition in GeV vs. sampling depth for hadronic showers.

Figure 18: Most probable value of the total signal vs. hadron energy.

Figure 19: Energy resolution vs. hadron energy.

Figure 20: Resolution of the projected angle vs. hadron energy.

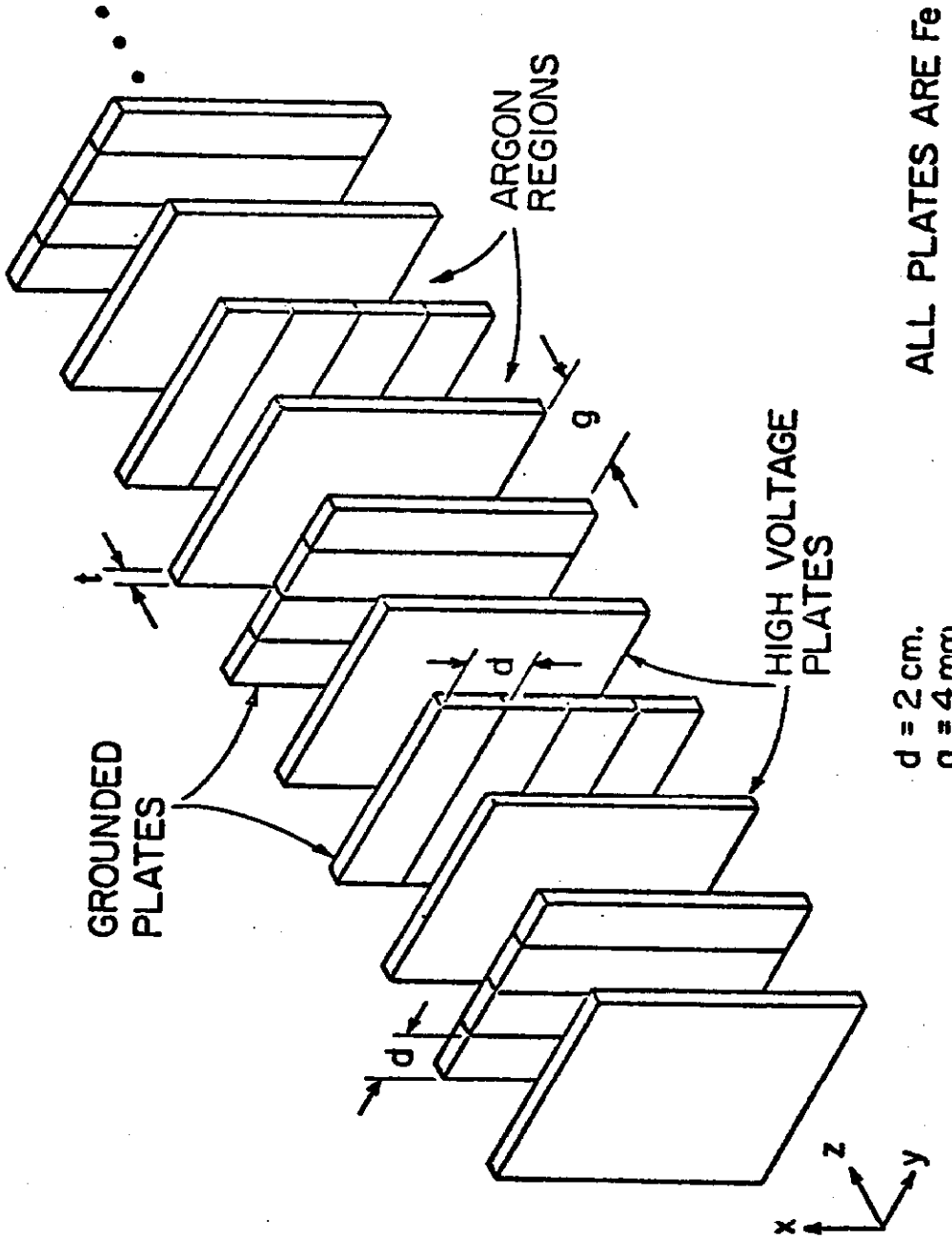
ARGON REGIONS
g
t
d
HIGH VOLTAGE PLATES
GROUNDED PLATES
d
z
y
x
ALL PLATES ARE Fe
d = 2 cm.
g = 4 mm
t = 3 mm

Fig. 1

Fig. 2

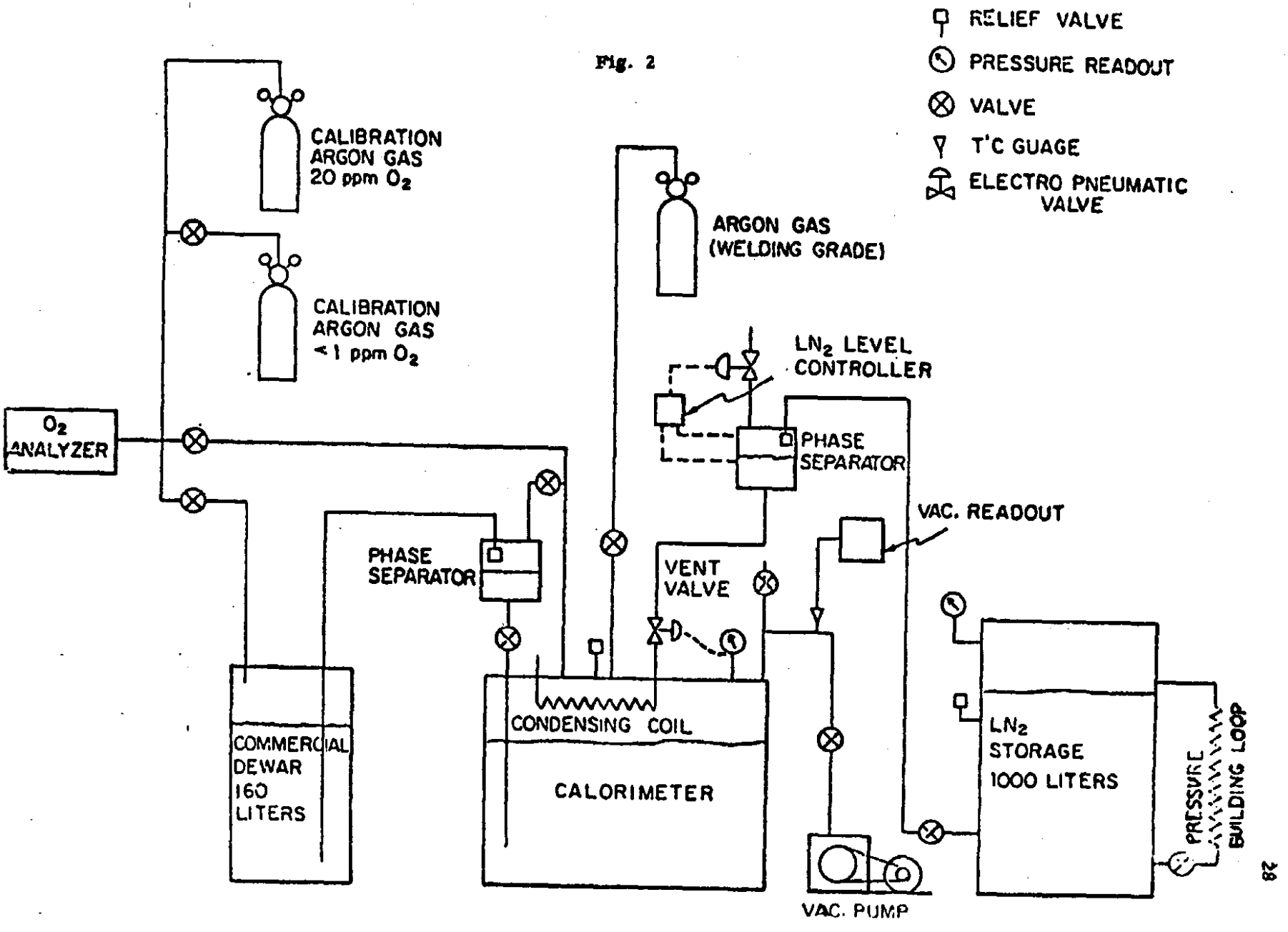
RELIEF VALVE
PRESSURE READOUT
VALVE
T'C GUAGE
ELECTRO PNEUMATIC VALVE
CALIBRATION ARGON GAS 20 ppm O_2
CALIBRATION ARGON GAS < 1 ppm O_2
ARGON GAS (WELDING GRADE)
LN_2 LEVEL CONTROLLER
O_2 ANALYZER
PHASE SEPARATOR
PHASE SEPARATOR
VAC. READOUT
VENT VALVE
COMMERCIAL DEWAR 160 LITERS
CONDENSING COIL
CALORIMETER
LN_2 STORAGE 1000 LITERS
PRESSURE BUILDING LOOP
VAC. PUMP

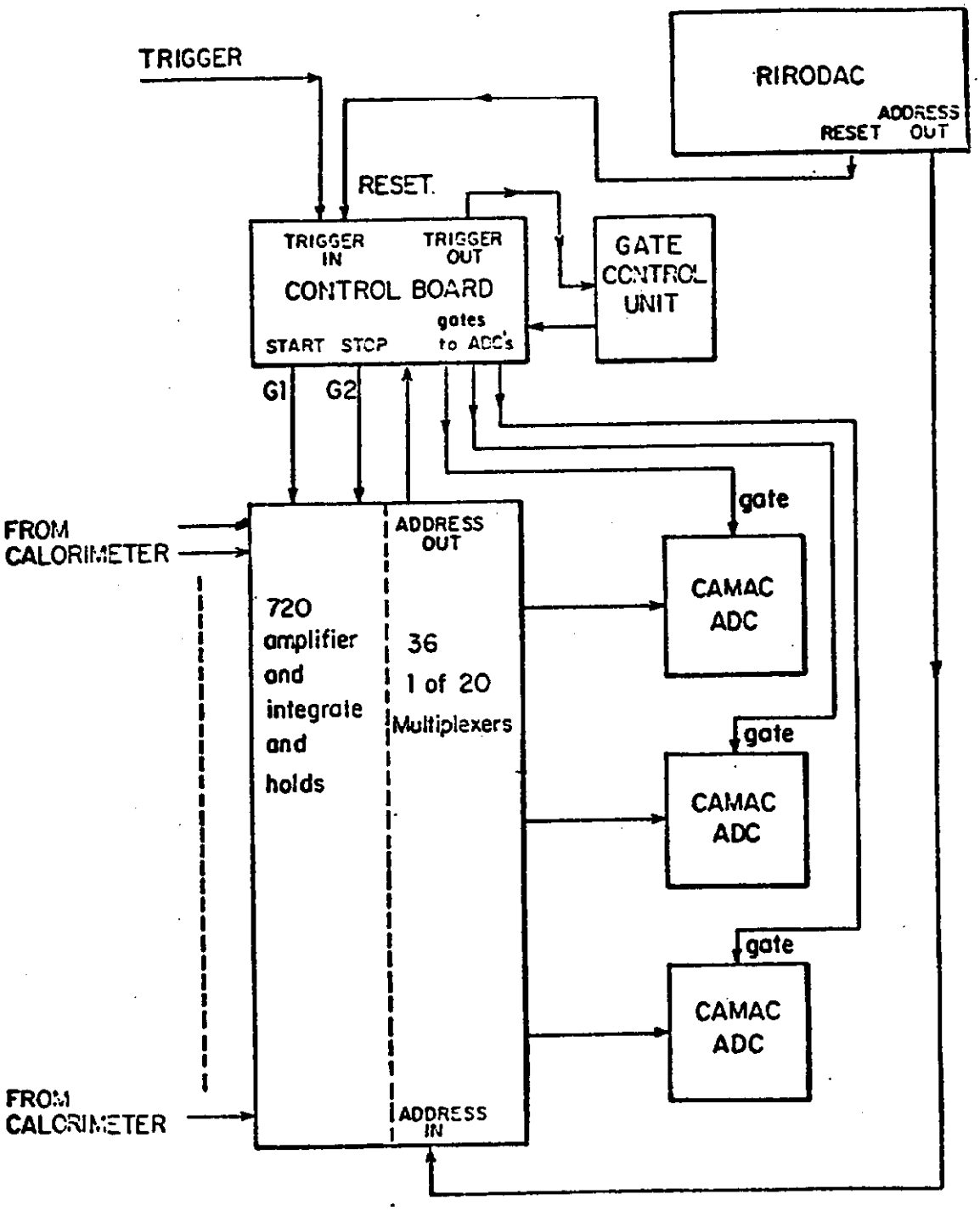
TRIGGER
RIRODAC
ADDRESS
RESET OUT
RESET
TRIGGER IN
TRIGGER OUT
CONTROL BOARD
START STOP
gates to ADC's
GATE CONTROL UNIT
G1
G2
gate
FROM CALORIMETER
ADDRESS OUT
720 amplifier and integrate and holds
36 1 of 20 Multiplexers
CAMAC ADC
gate
CAMAC ADC
gate
CAMAC ADC
FROM CALORIMETER
ADDRESS IN

Fig. 3

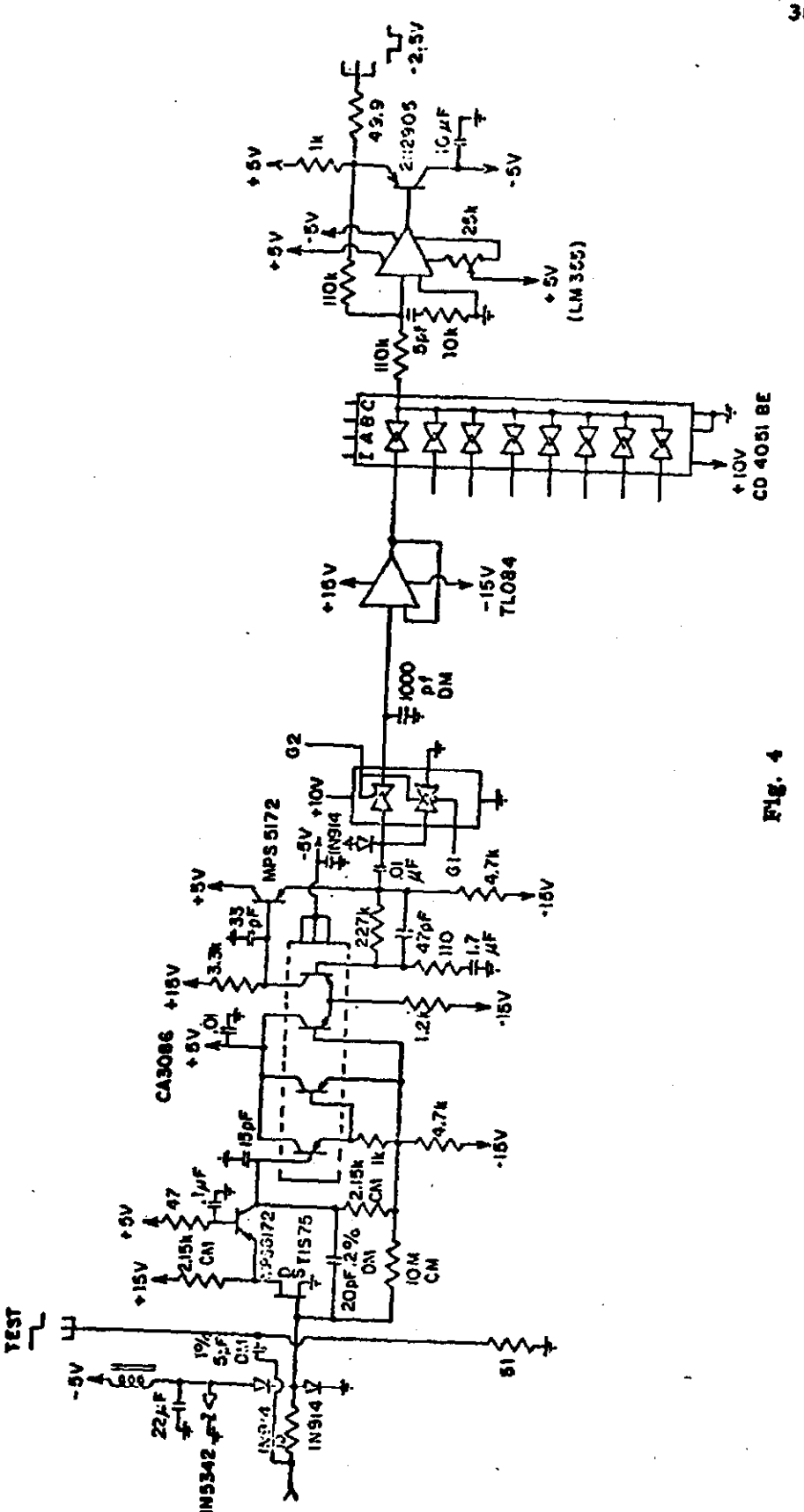
-2.5V
49.9
2N2905
1k
+5V
10µF
-5V
25k
110k
5pF
10k
+5V (LM 355)
CD 4051 BE
+10V
+15V
-15V
TL084
1000 pf
G2
G1
MPS 5172
IN914
.01 µF
4.7k
33 pF
3.3k
227k
47pF
110
1.7 µF
1.2k
CA3086
.1
15pF
2.15k
47
.1µF
TIS75
20pF 2%
10M
TEST
1%
51
22µF
IN5342
IN914

Fig. 4

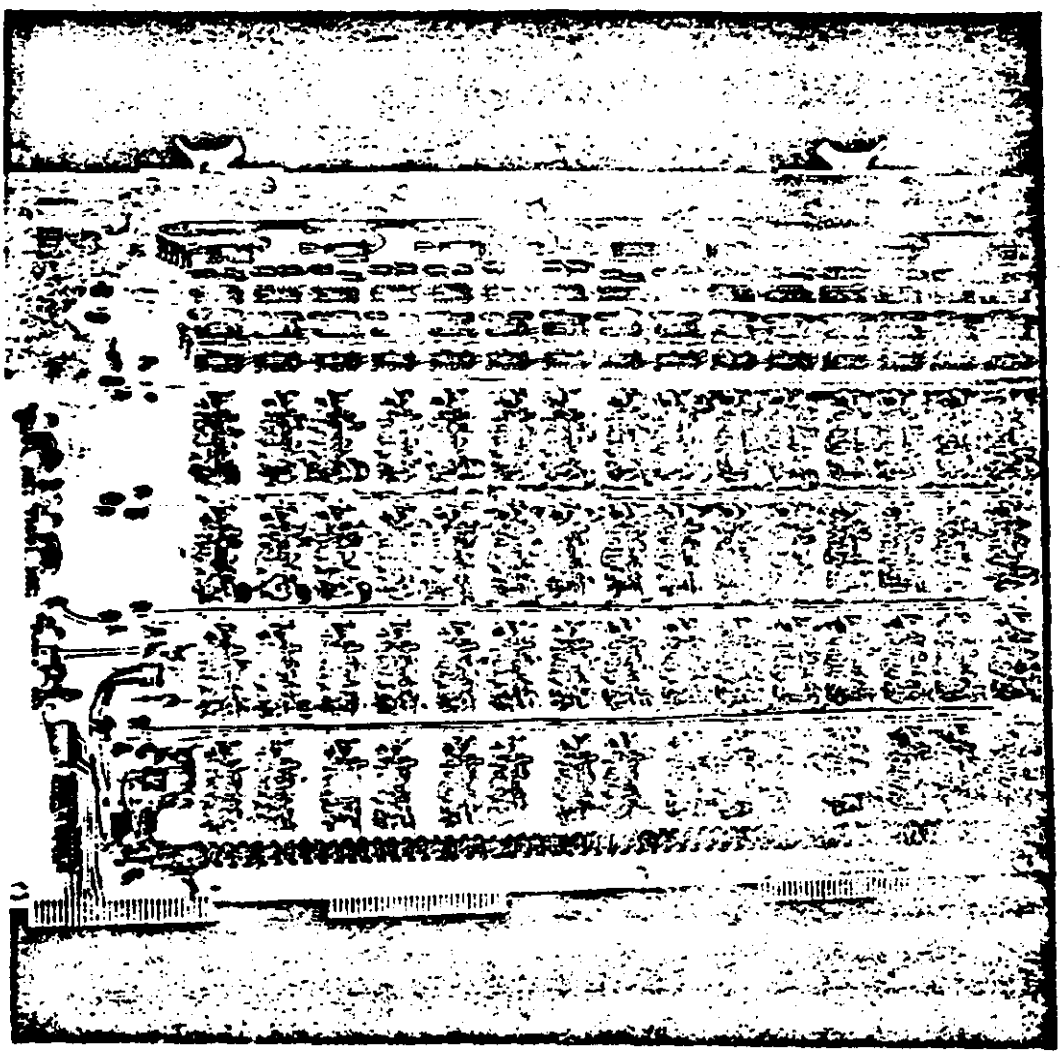

Fig. 5

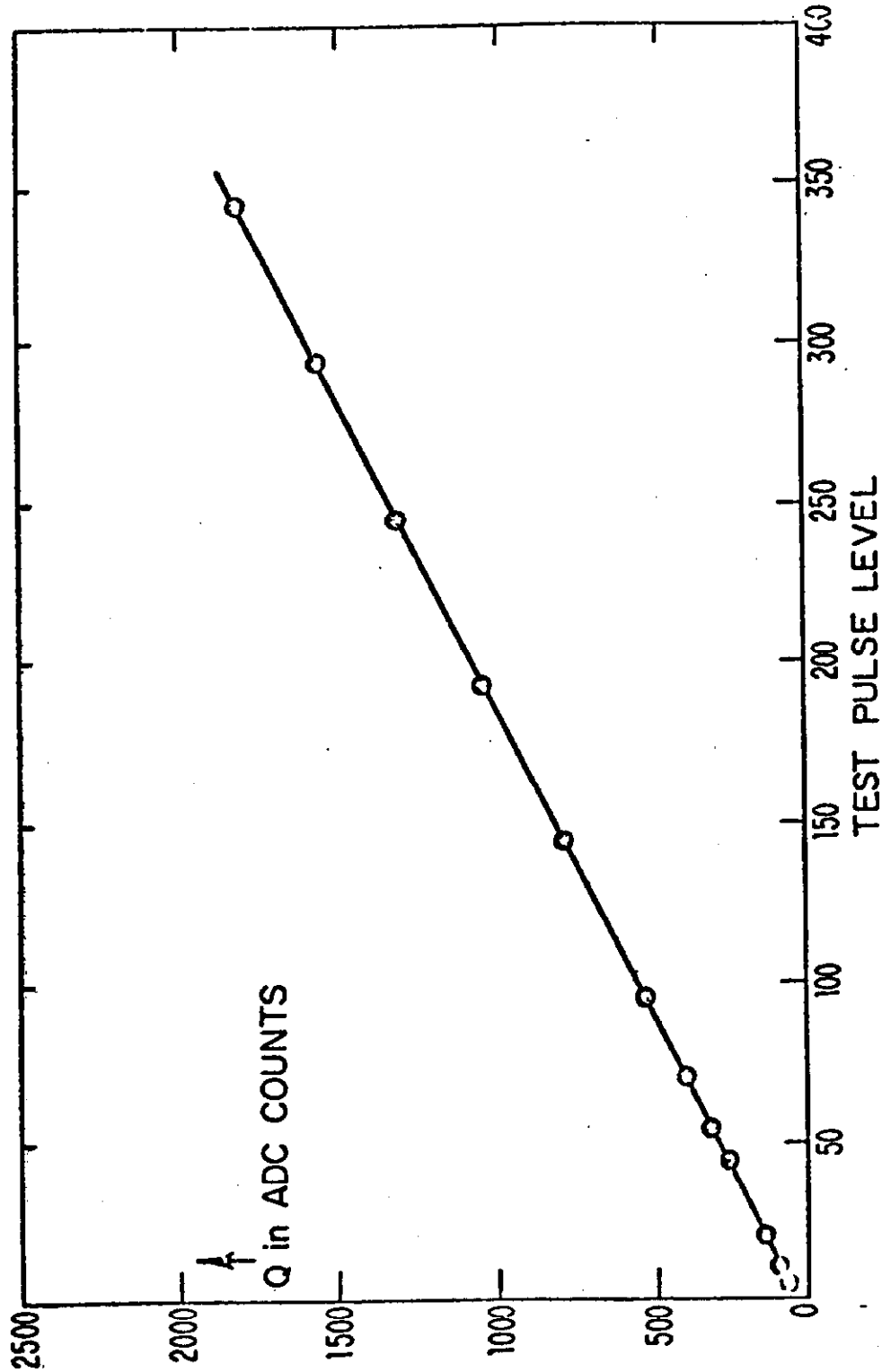
2500
2000
1500
1000
500
0
Q in ADC COUNTS
50
100
150
200
250
300
350
400
TEST PULSE LEVEL

Fig. 6

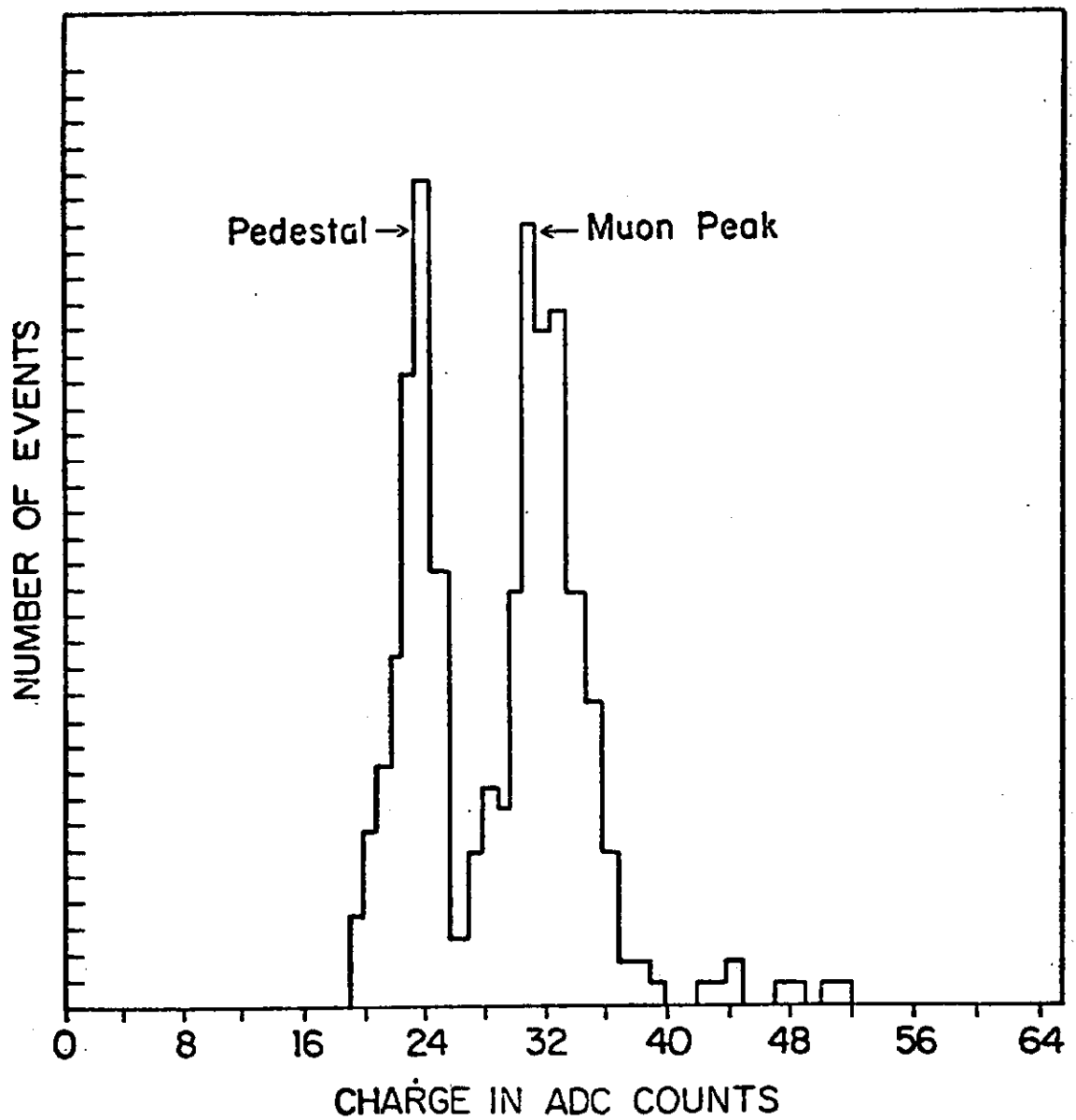
Pedestal →
← Muon Peak
NUMBER OF EVENTS
0
8
16
24
32
40
48
56
64
CHARGE IN ADC COUNTS

Fig. 7

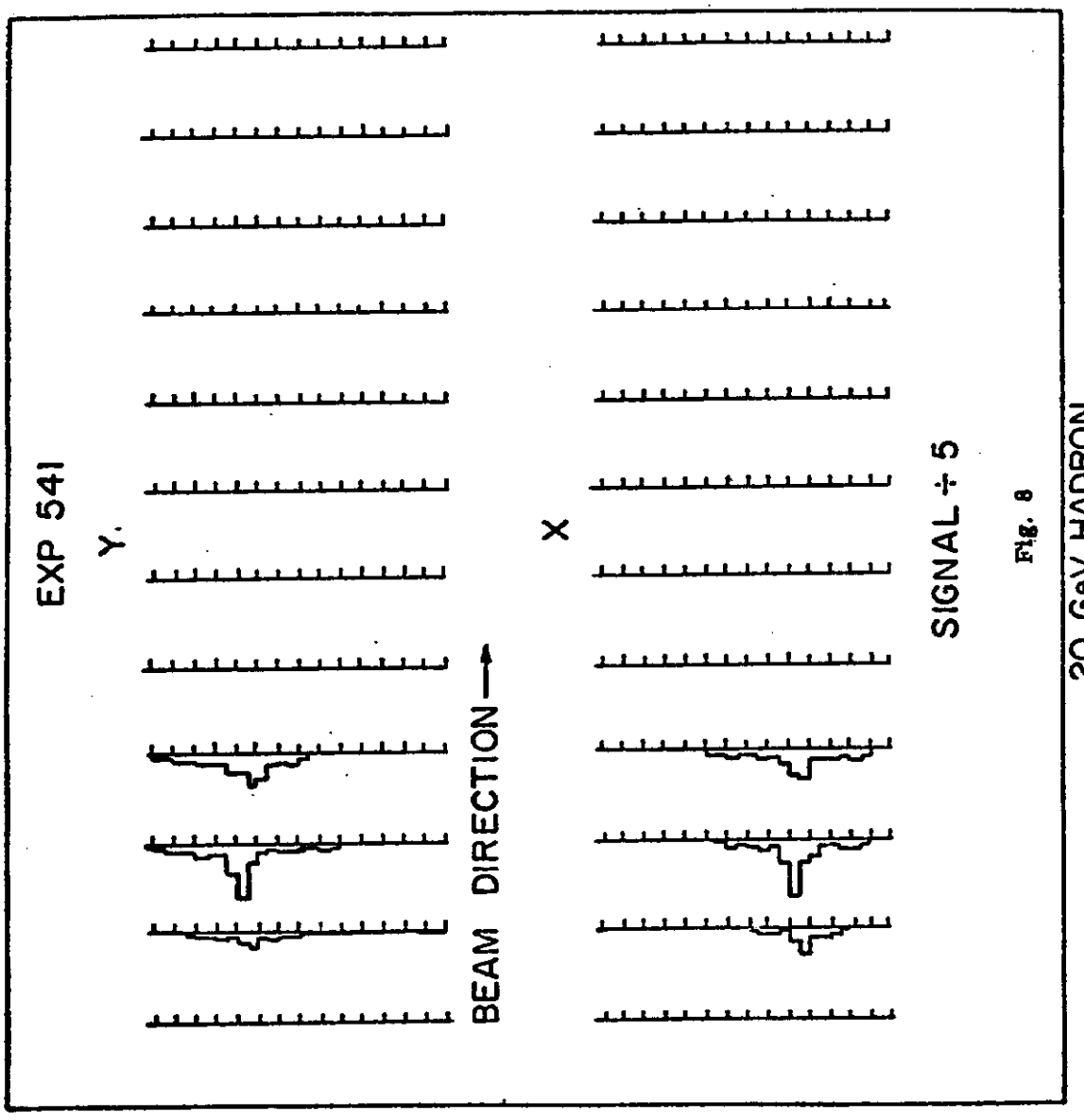

Fig. 8

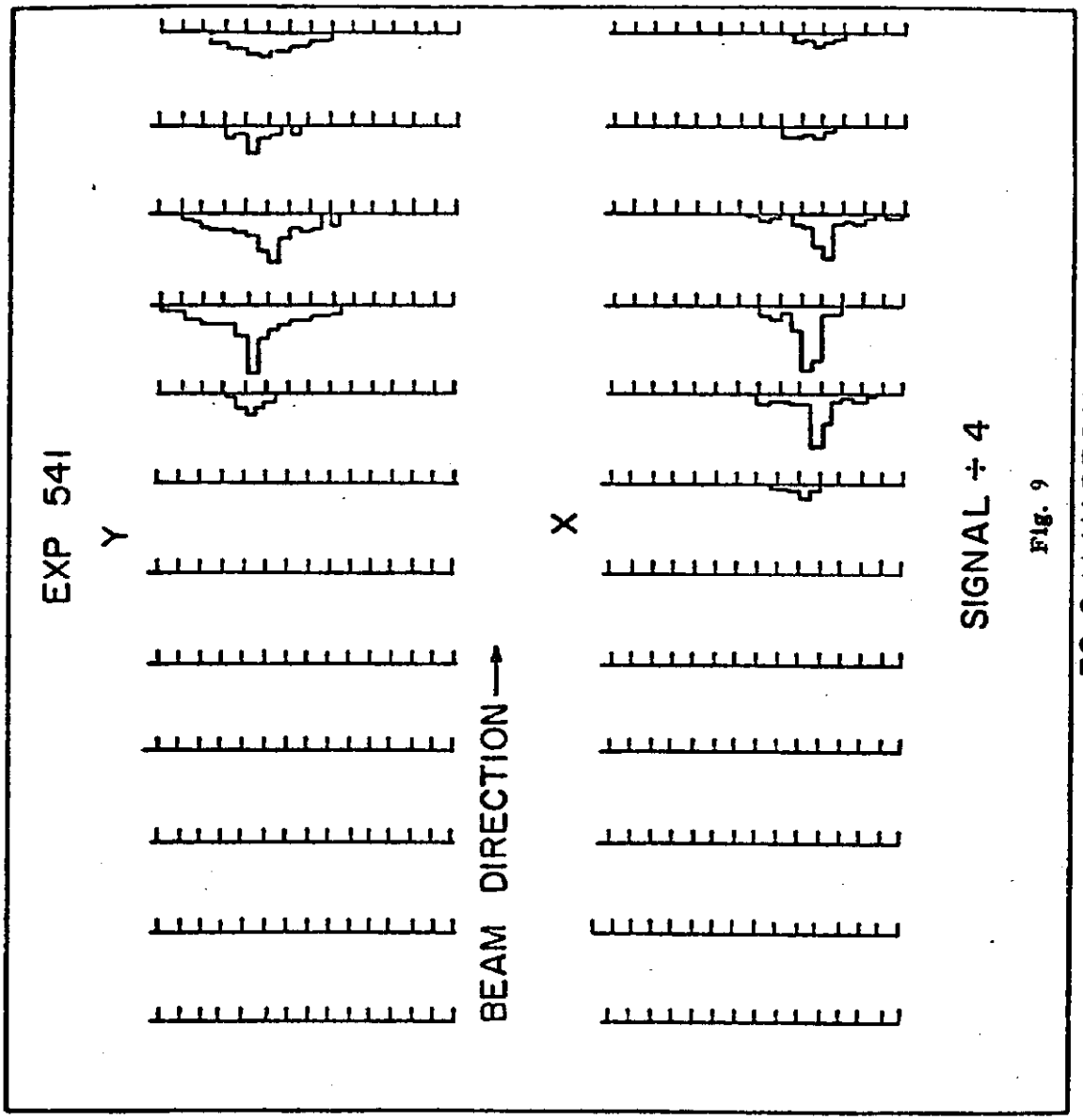

Fig. 9

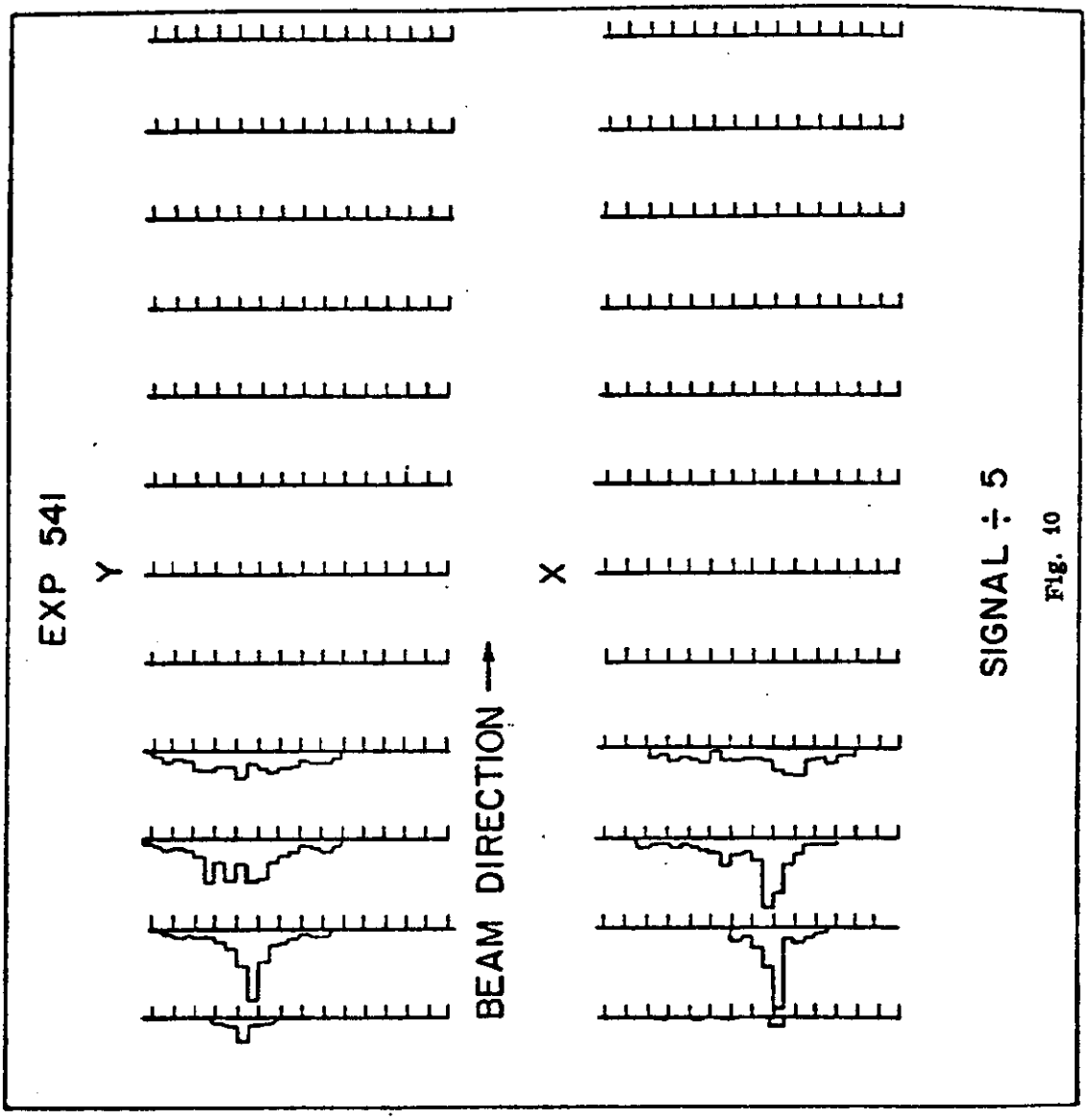

Fig. 10

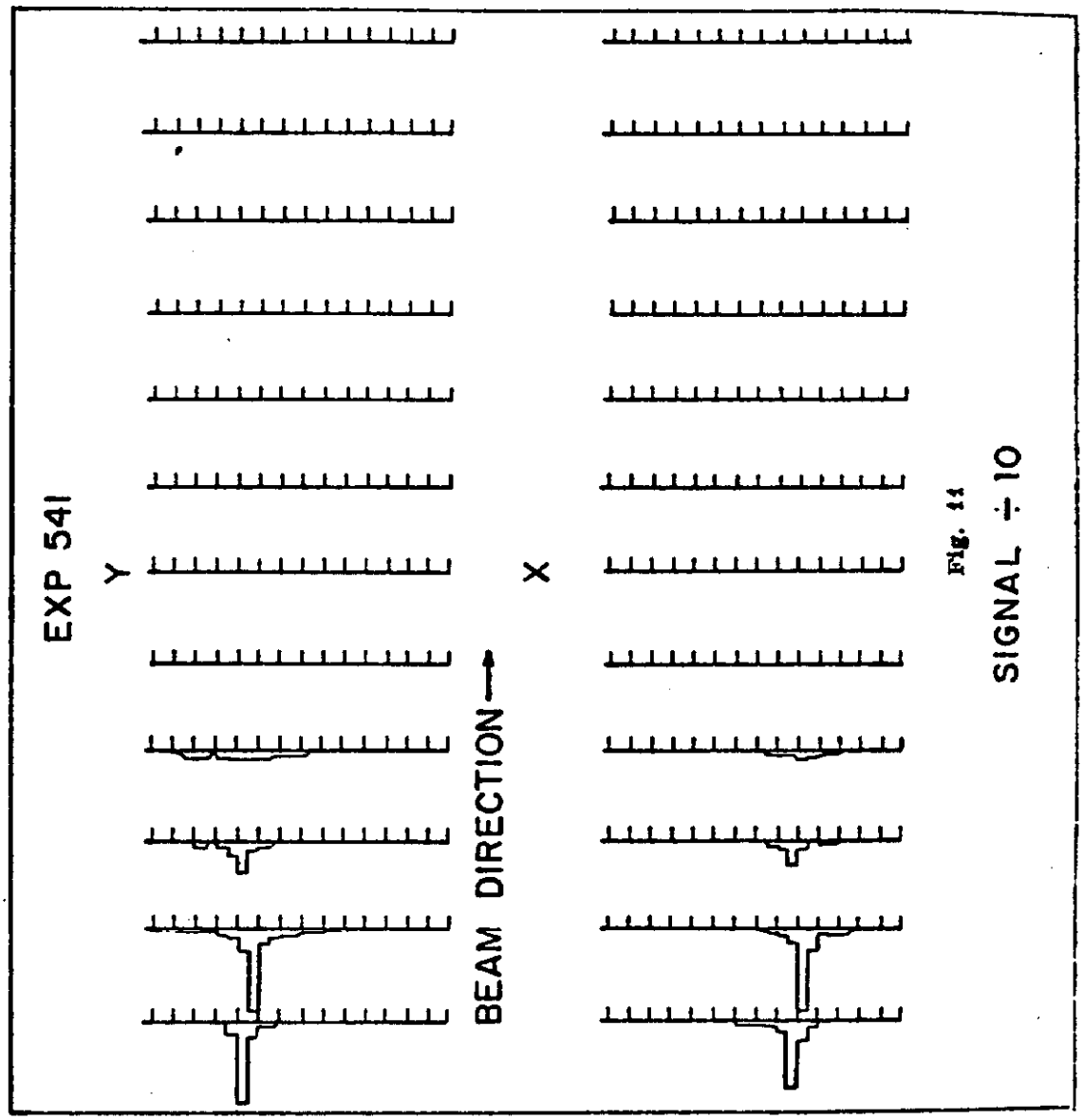

Fig. 11

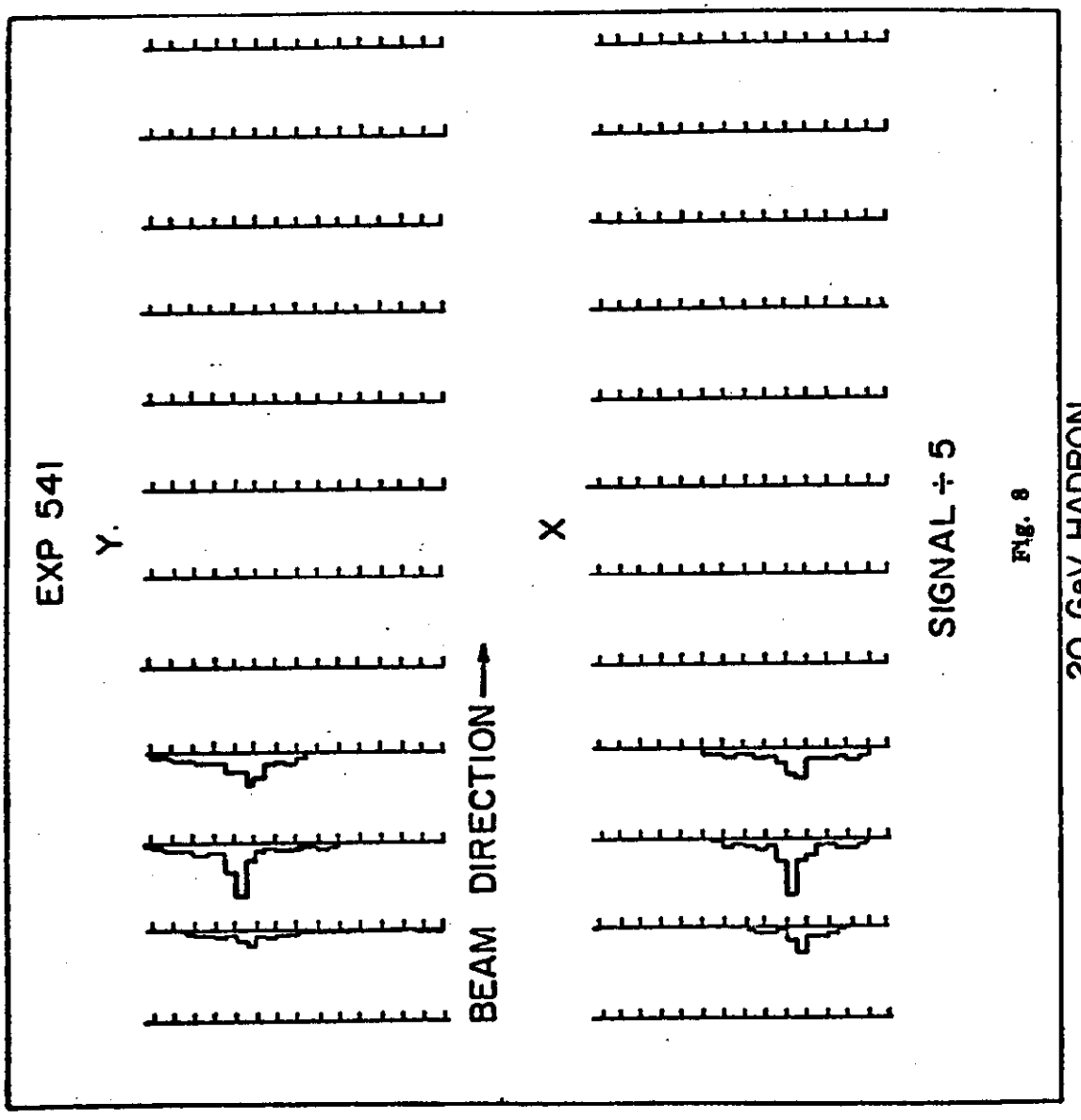

Fig. 8

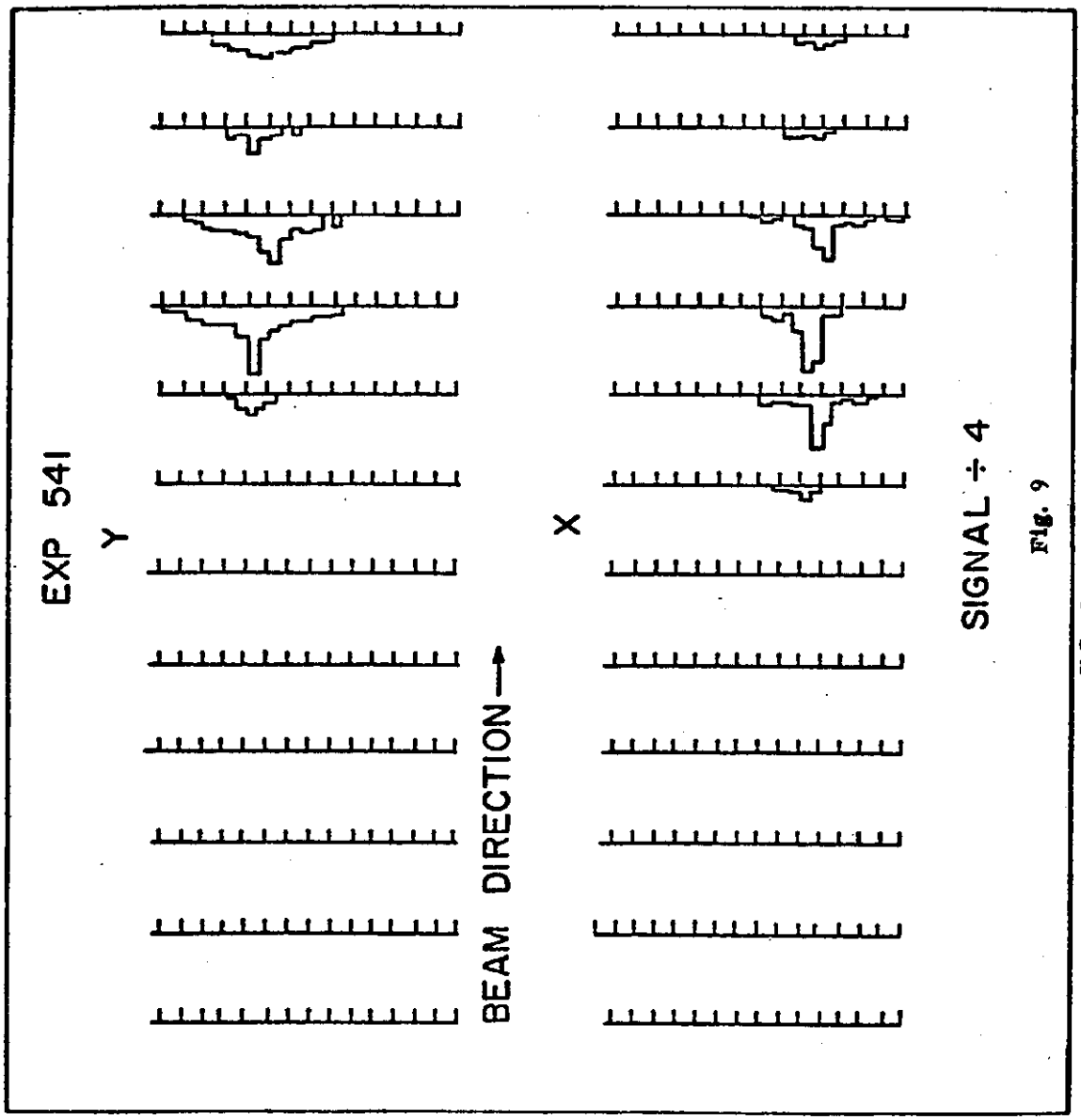

Fig. 9

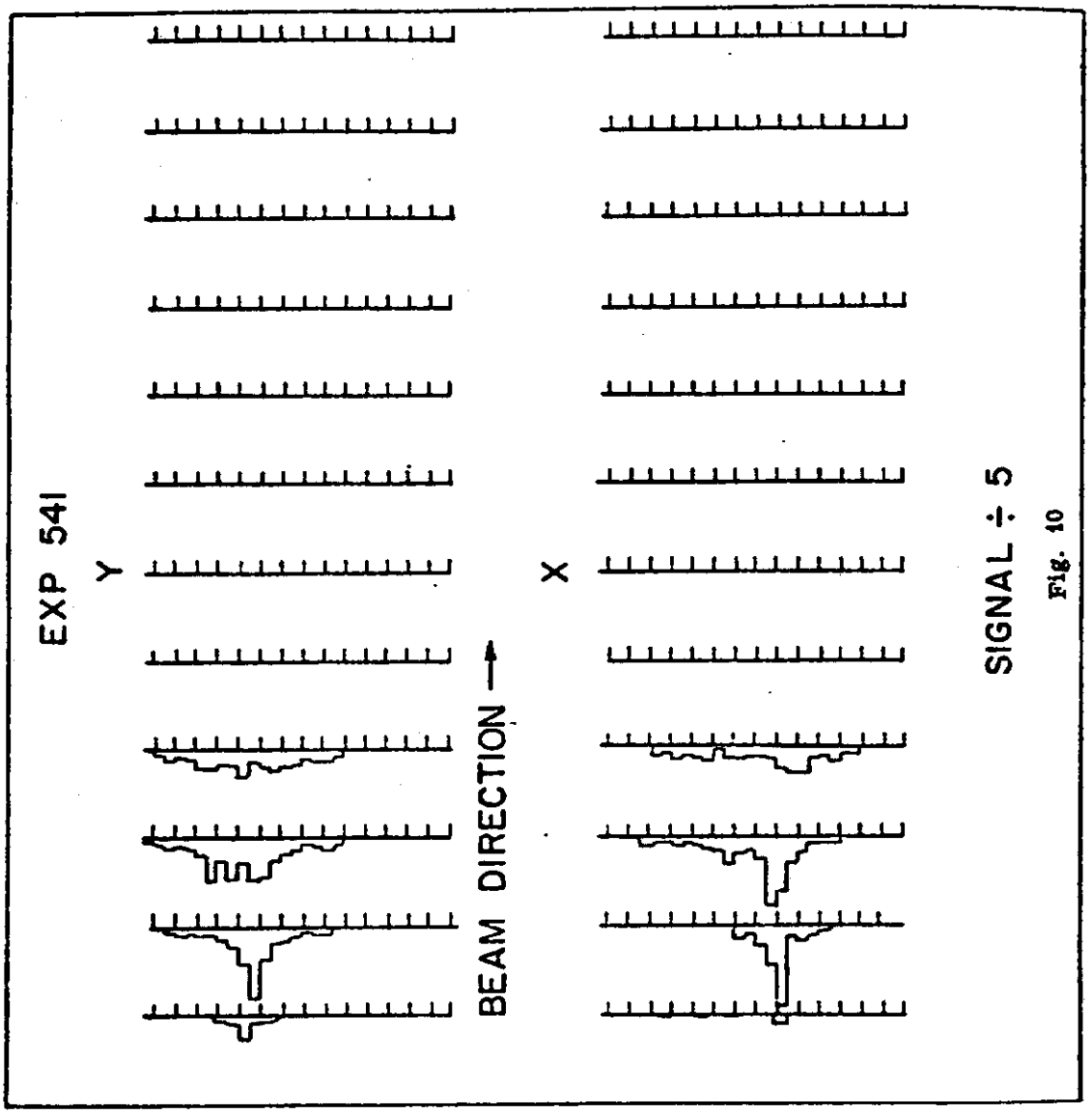

Fig. 10

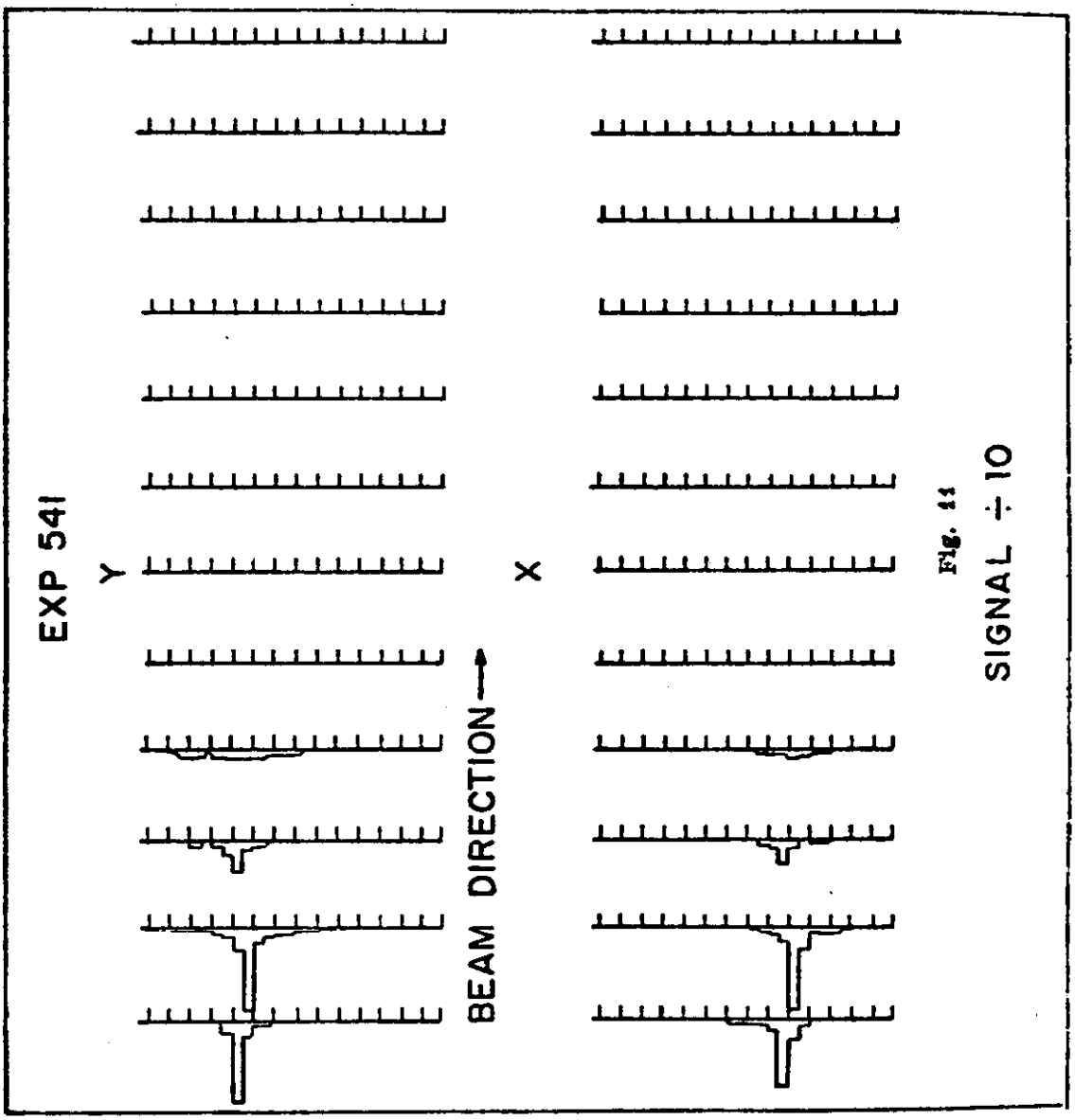

Fig. 11

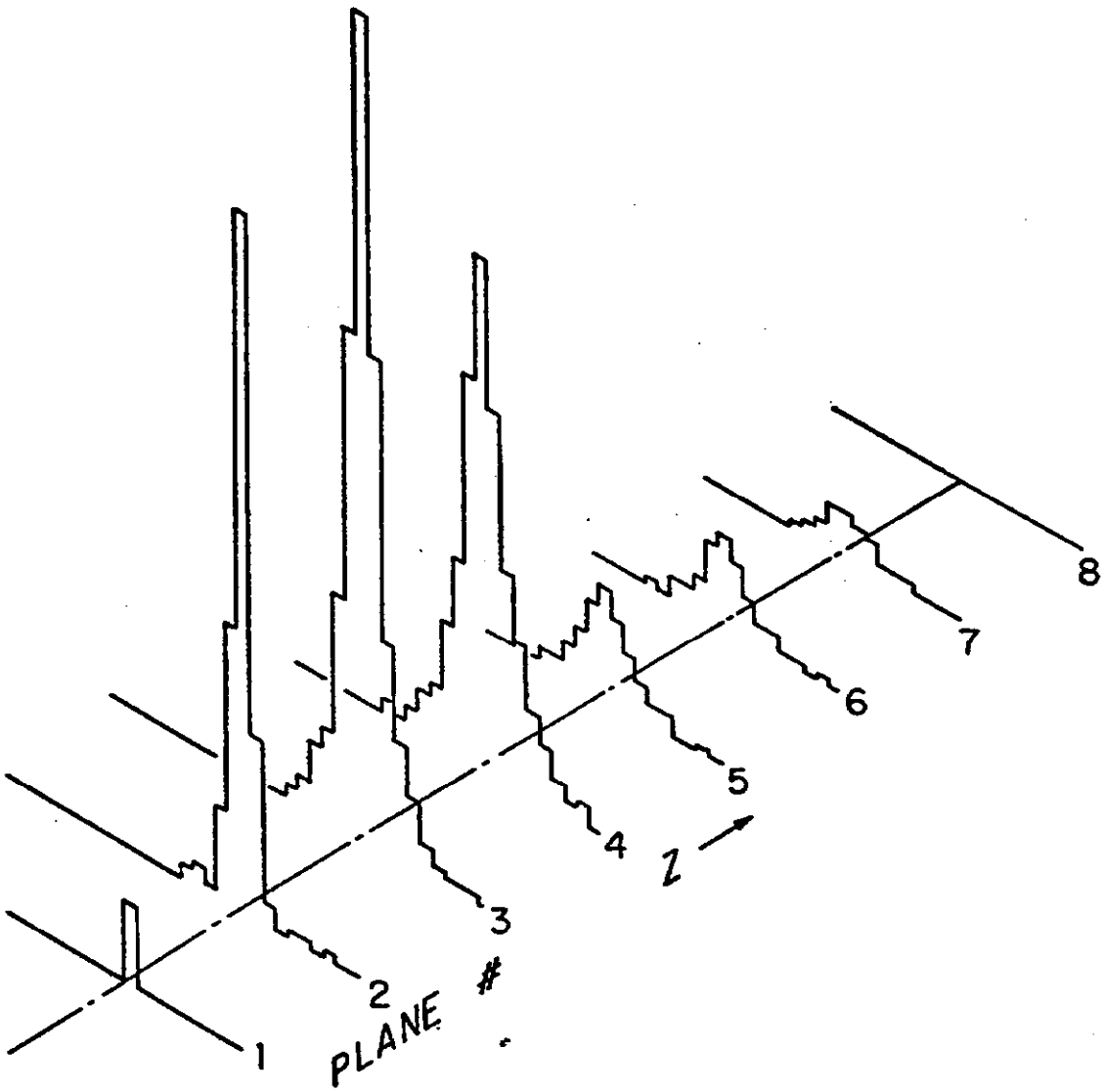

Fig. 12

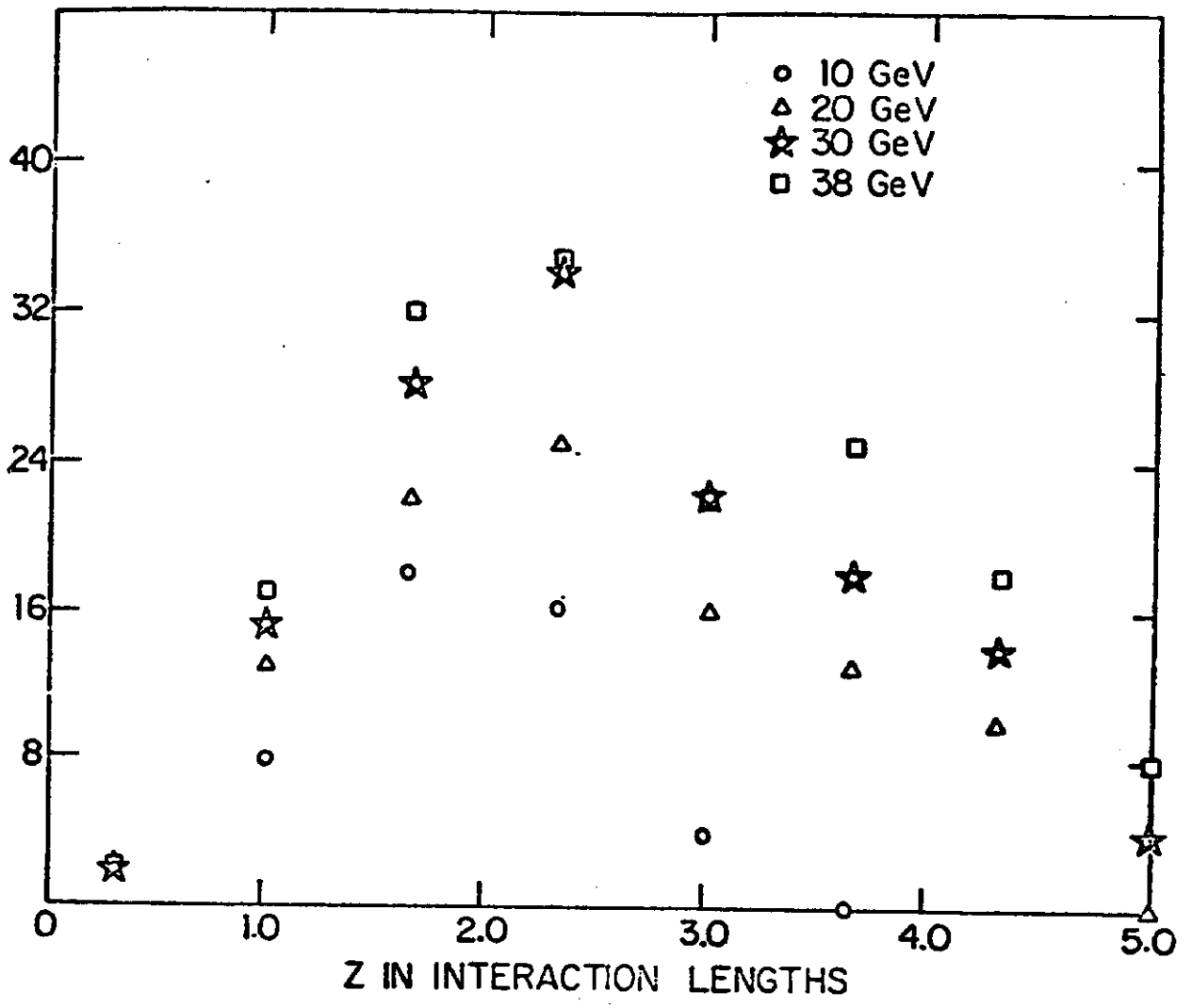
10 GeV
20 GeV
30 GeV
38 GeV
40
32
24
16
8
0
1.0
2.0
3.0
4.0
5.0
Z IN INTERACTION LENGTHS

Fig. 13

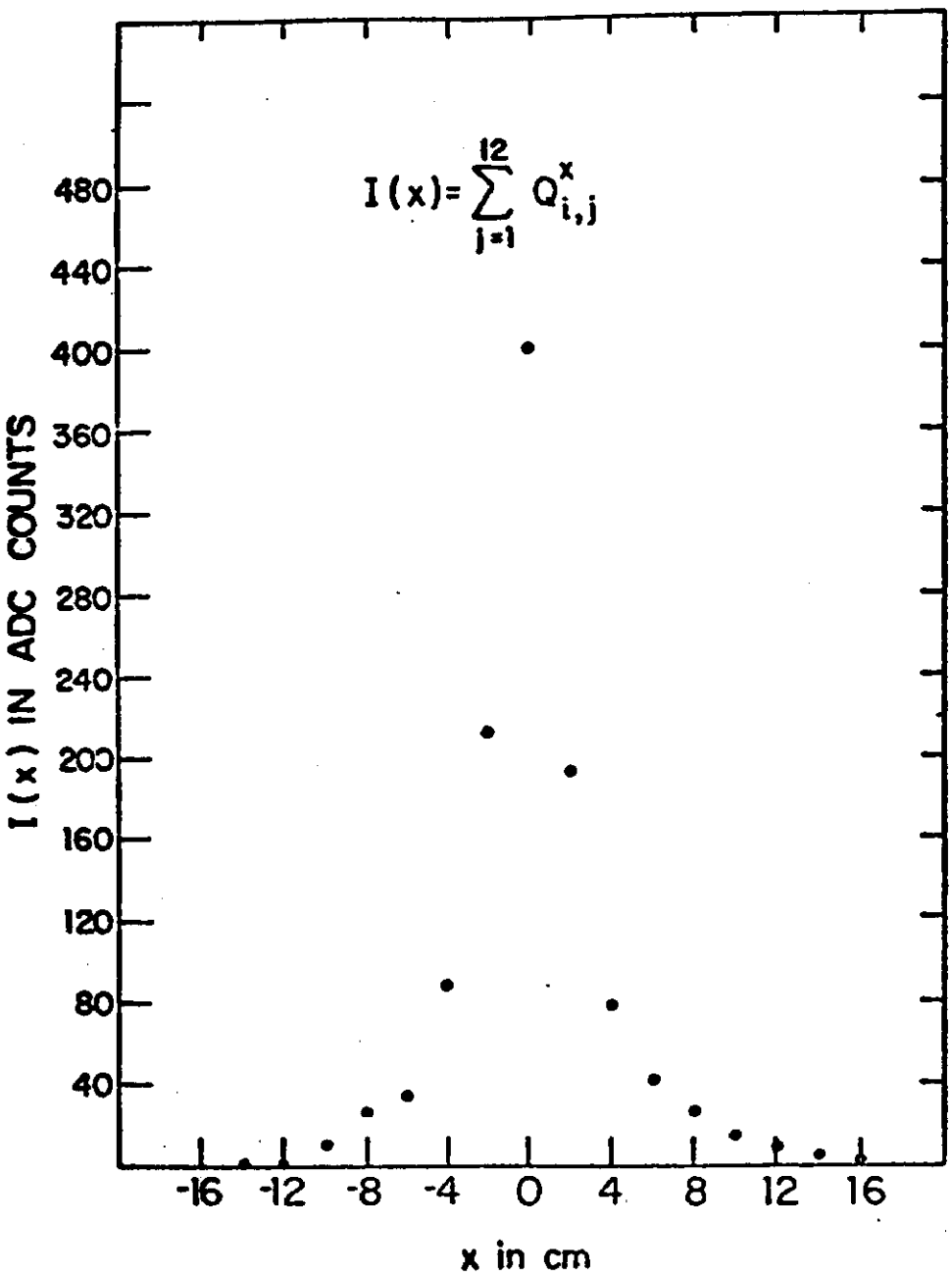
$I(x)=\sum_{j=1}^{12} Q_{i,j}^{x}$
I(x) IN ADC COUNTS
480
440
400
360
320
280
240
200
160
120
80
40
-16
-12
-8
-4
0
4
8
12
16
x in cm

Fig. 14

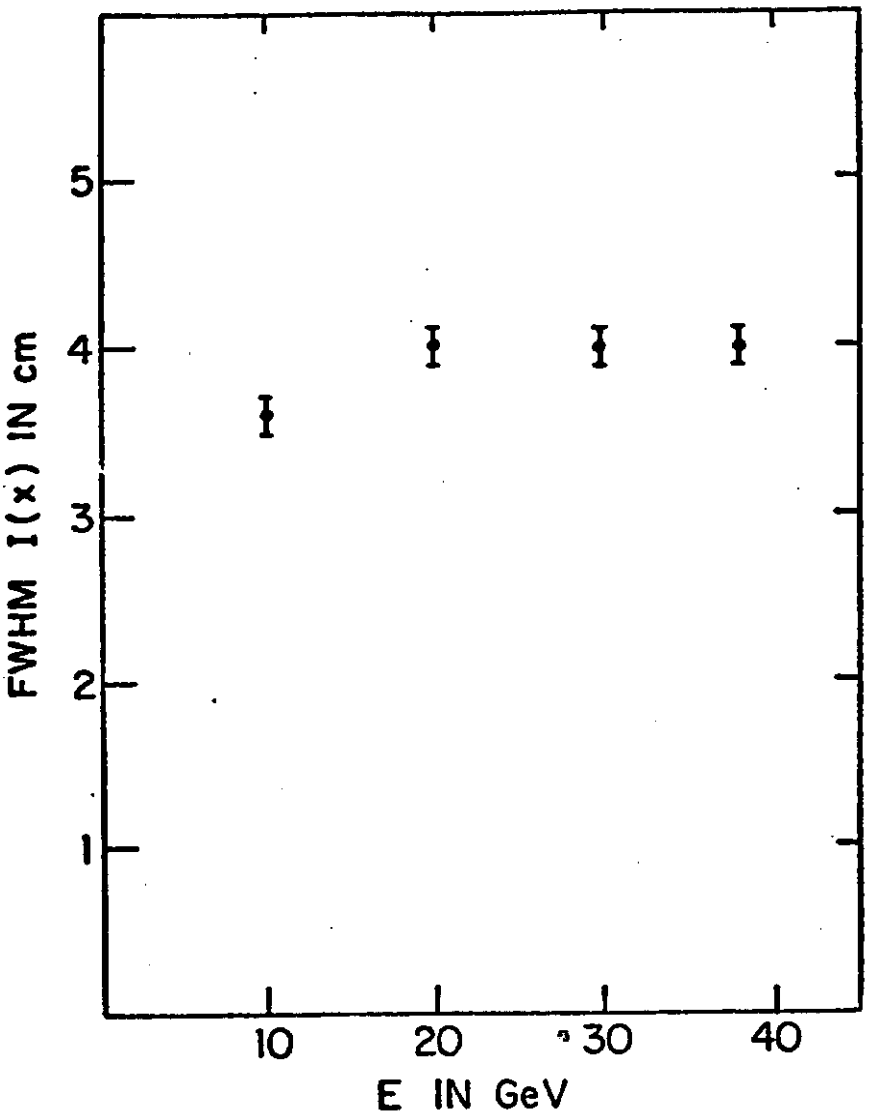

Fig. 15

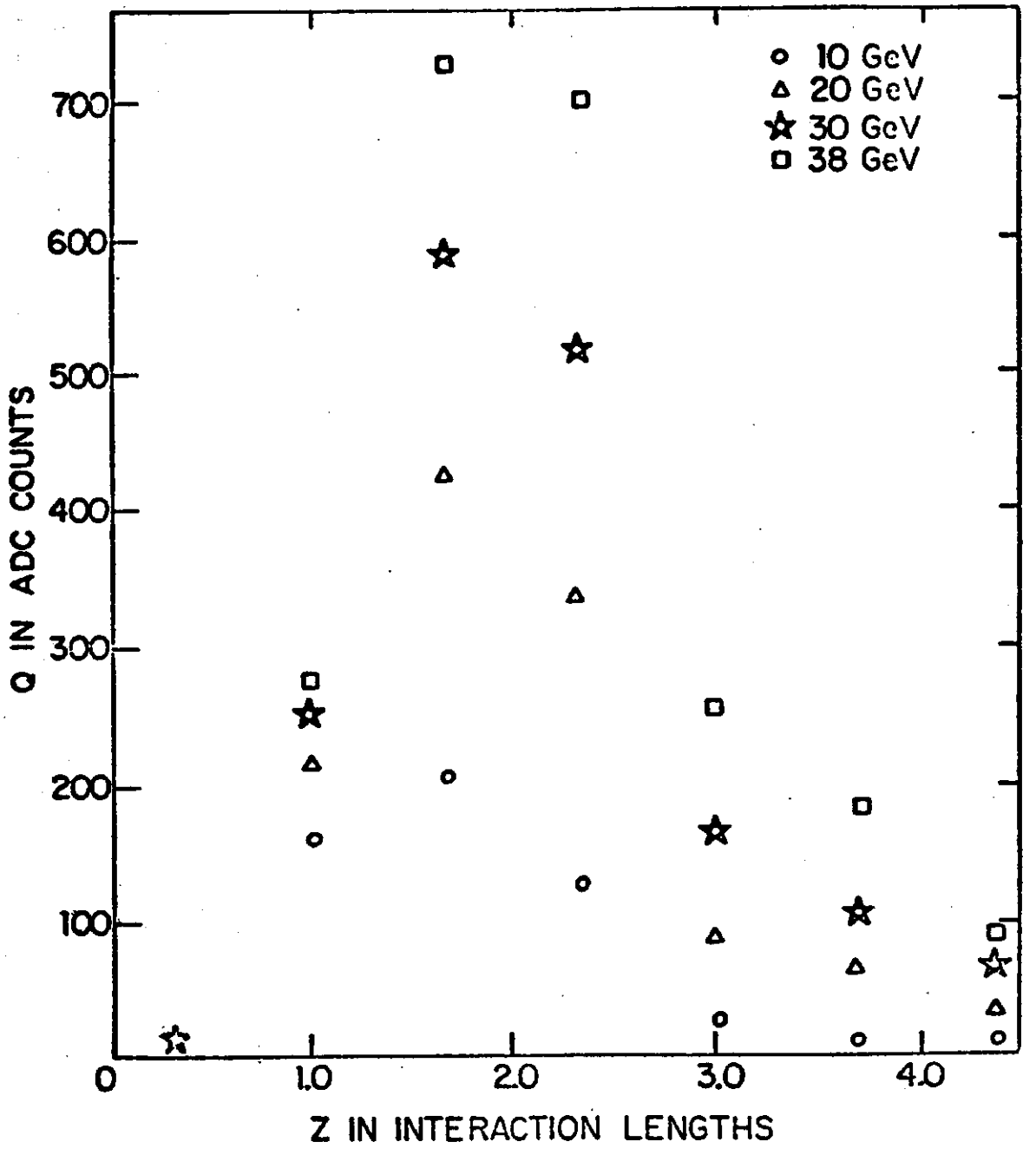
10 GeV
20 GeV
30 GeV
38 GeV
Q IN ADC COUNTS
Z IN INTERACTION LENGTHS
0
1.0
2.0
3.0
4.0
100
200
300
400
500
600
700

Fig. 16

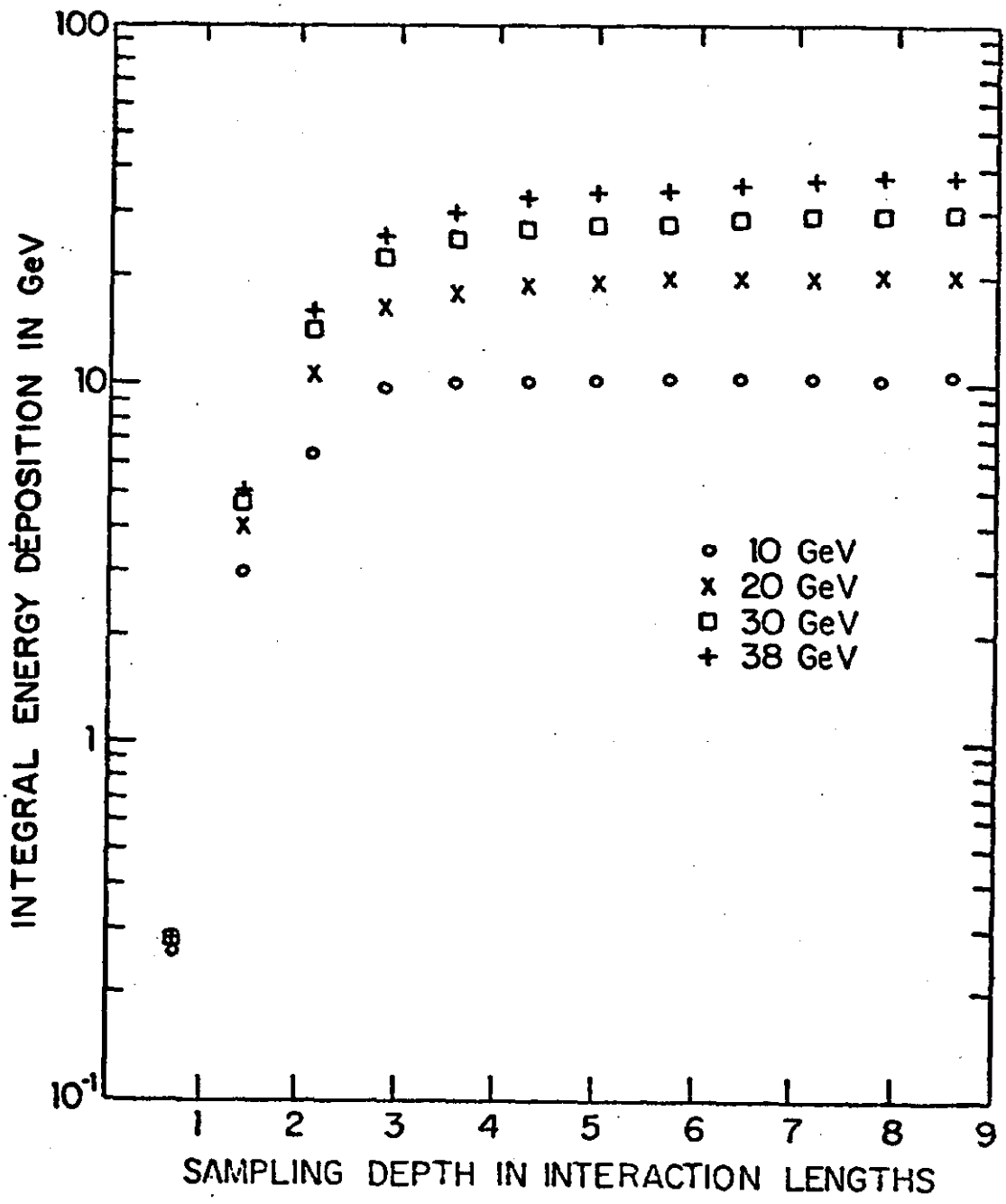
100
10
1
10^{-1}
INTEGRAL ENERGY DEPOSITION IN GeV
1
2
3
4
5
6
7
8
9
SAMPLING DEPTH IN INTERACTION LENGTHS
10 GeV
20 GeV
30 GeV
38 GeV

Fig. 17

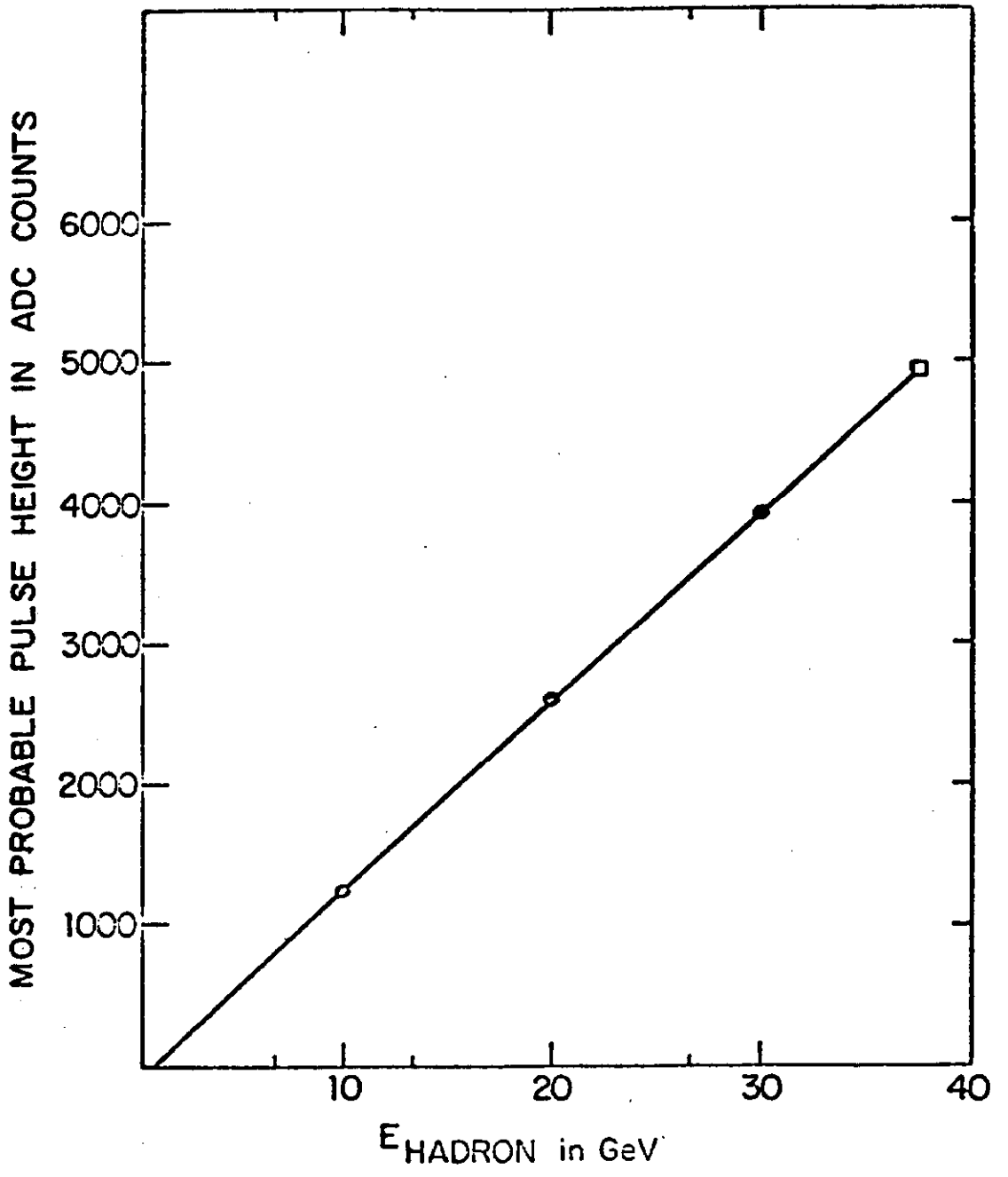
MOST PROBABLE PULSE HEIGHT IN ADC COUNTS
6000
5000
4000
3000
2000
1000
10
20
30
40
E HADRON in GeV

Fig. 18

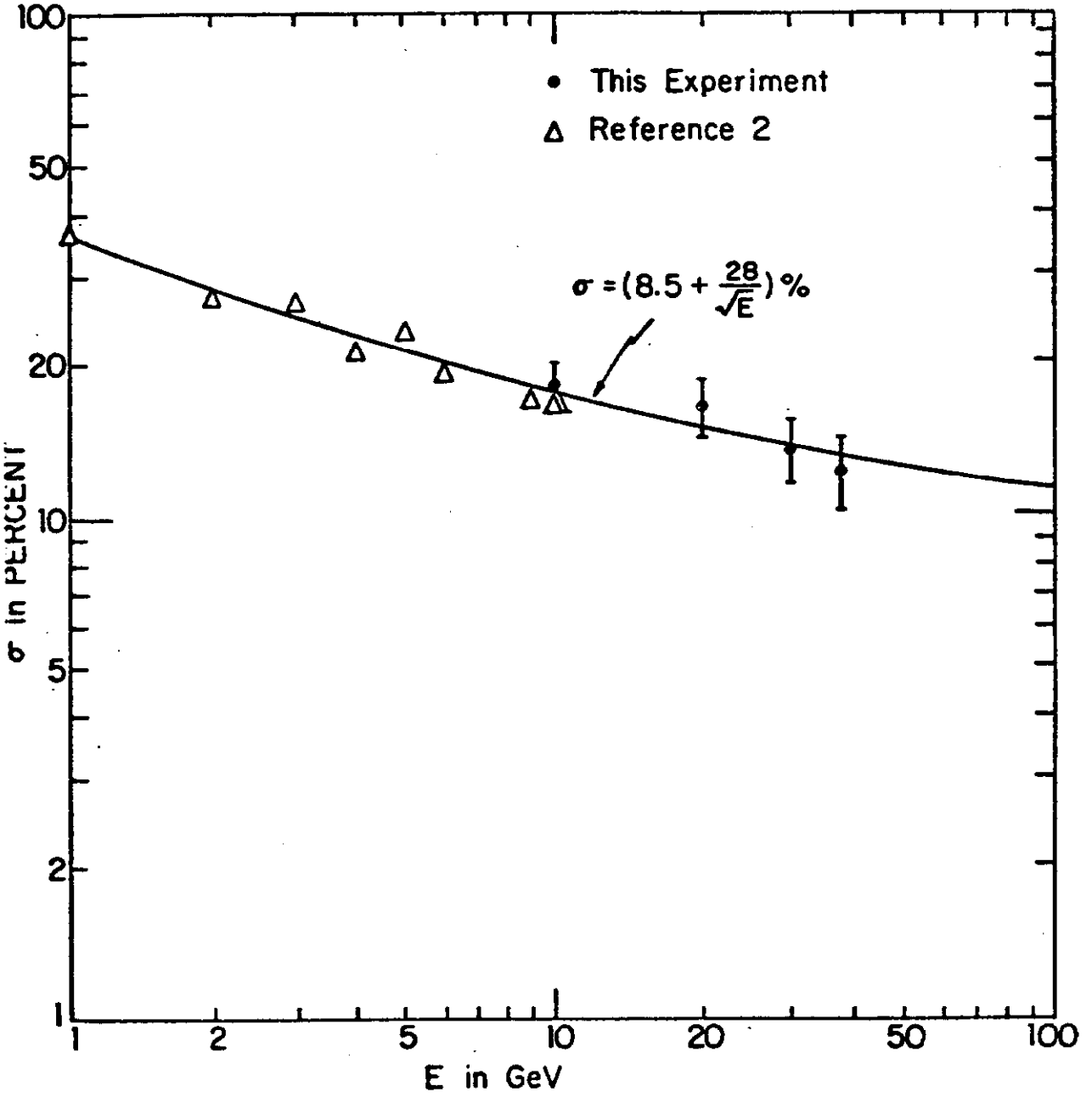
100
50
20
10
5
2
1
σ in PERCENT
• This Experiment
Δ Reference 2
σ = (8.5 + 28/√E) %
1
2
5
10
20
50
100
E in GeV

Fig. 19

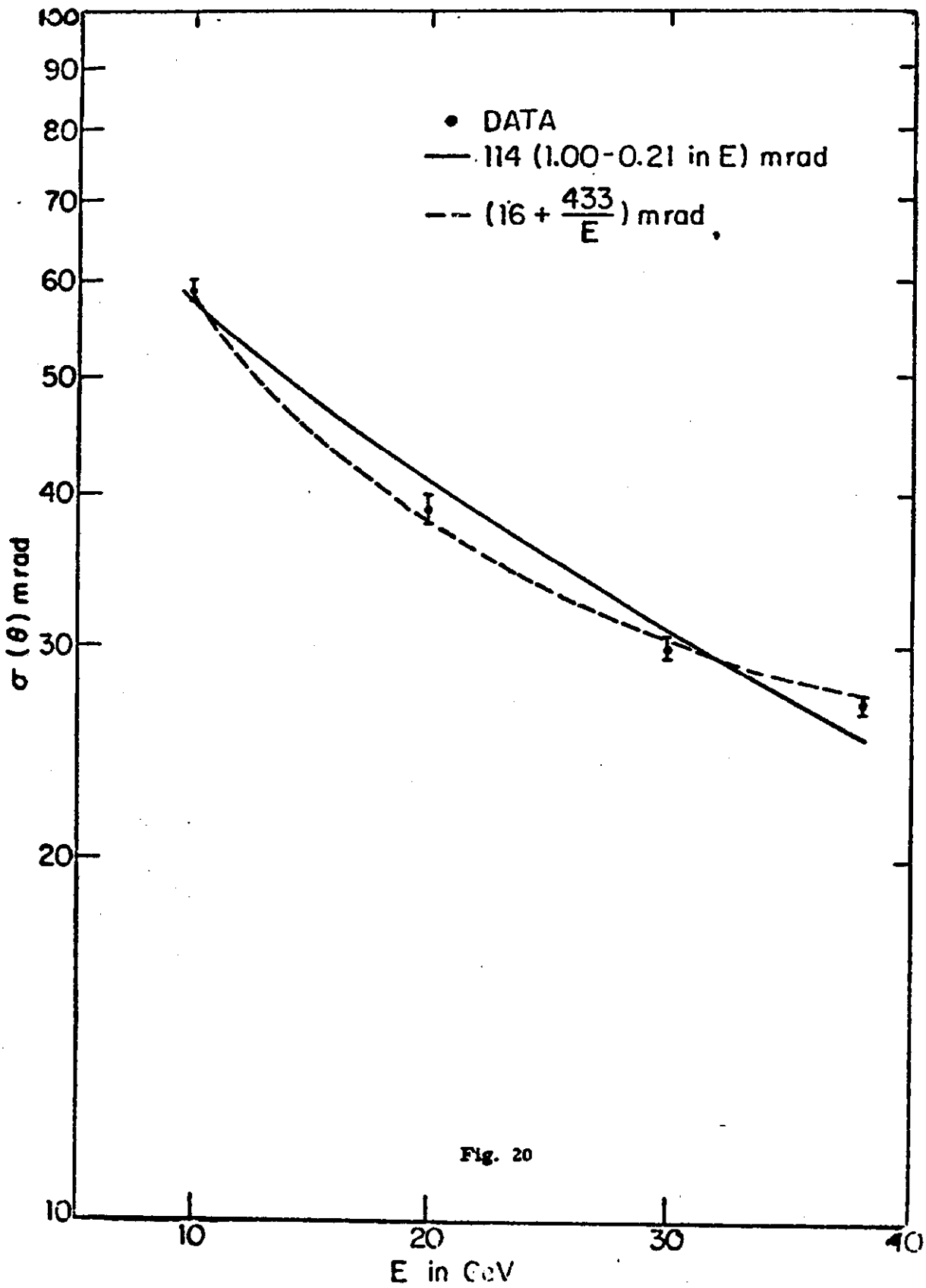
• DATA
— 114 (1.00-0.21 in E) mrad
-- (16 + 433/E) mrad
σ (θ) mrad
E in GeV
100
90
80
70
60
50
40
30
20
10
10
20
30
40

Fig. 20